CDF/ANAL/BOTTOM/CDFR/7420
Revision 3.0

Study of $b\bar{b}$ Background in $B_c^{\pm} \rightarrow \mathrm{J}/\psi + \mu^{\pm} + \mathrm{X}$ with Run II Data

Mark Hartz, Paul Shepard, Turgun Nigmanov

University of Pittsburgh

June, 2005

1 Introduction

One of the backgrounds for measuring the B_c signal in the $B_c^{\pm} \rightarrow \mathrm{J}/\psi + \mu^{\pm} + \mathrm{X}$ decay channel are $b\bar{b}$ events. These are events where one or more pairs of b quarks are created with one quark eventually decaying to a J/ψ and the other to a $\mu^{\pm}$. To estimate the number of $b\bar{b}$ background events in B_c candidates we generate a Pythia Monte Carlo (MC) sample of 50 million events containing $b\bar{b}$ pairs and apply the B_c cuts. To normalize the $b\bar{b}$ background events from the Pythia sample to data, we use the $B^{\pm} \rightarrow \mathrm{J}/\psi + \mathrm{K}^{\pm}$ peaks in data and Pythia. This calculation is sensitive to two corrections. First we must correct for the production cross section of $B^{\pm}$ (as a fraction of all B production) and the decay fraction of $B^{\pm} \rightarrow \mathrm{J}/\psi + \mathrm{K}^{\pm}$ in Pythia to match the measured values. Secondly we must correct the Pythia sample for the relative fraction of $b\bar{b}$ productions mechanisms as the production mechanisms have differing distributions of $\Delta\phi$, the azimuthal angle, between b quark pairs. Since the B_c analysis includes a cut on the J/ψ+$\mu^{\pm}$ $\Delta\phi$ the final answer is sensitive to the relative fraction of these production mechanisms.

2 Pythia B^{+} Correction

For the Pythia sample we use a user defined decay table to force all B hadrons coming from the b quark to decay to J/ψ, while B hadrons coming from $\bar{b}$ quarks are allowed to decay via the default decay table. We also create a custom J/ψ for the forced B decays which is then forced to decay to two muons. To ensure the correct normalization using the $B^{\pm} \rightarrow$ J/ψ + K$^{\pm}$ peak, we make sure that data and Pythia have the same number of J/ψ per $B^{\pm} \rightarrow$ J/ψ + K$^{\pm}$. In terms of the fractional production cross section for $B^{\pm}$, F($B^{\pm}$), the branching fraction, F($B^{\pm} \rightarrow$ J/ψ + K$^{\pm}$), and the branching fraction for all B hadrons, F($H_b \rightarrow$ J/ψ + X), we have the requirement:

$$\frac{F_{data}(B^{\pm}) * F_{data}(B^{\pm} \rightarrow \mathrm{J}/\psi + \mathrm{K}^{\pm})}{F_{data}(H_b \rightarrow \mathrm{J}/\psi + \mathrm{X})} = \frac{F_{Pythia}(B^{+}) * F_{Pythia}(B^{+} \rightarrow \mathrm{J}/\psi + \mathrm{K}^{+})}{F_{Pythia}(H_b \rightarrow \mathrm{J}/\psi + \mathrm{X})} * C_{Norm}$$

C$_{Norm}$ is the correction factor we will calculate. Measured values for data are published in the PDG [1].

$$F_{data}(B^{\pm}) = 0.397 \pm 0.010$$
$$F_{data}(B^{\pm} \rightarrow \mathrm{J}/\psi + \mathrm{K}^{\pm}) = 0.00100 \pm 0.00004$$
$$F_{data}(H_b \rightarrow \mathrm{J}/\psi + \mathrm{X}) = 0.0116 \pm 0.0010$$

From the Pythia MC we can measure the fractional production cross section of B^{+}. We do this by taking an unfiltered Pythia sample and counting the number of B^{+} events generated and dividing by the total number of events with a B hadron from the b in the $b\bar{b}$ pair.

$$F_{Pythia}(B^{+}) = 0.455 \pm 0.004$$

The $B^{+} \rightarrow$ J/ψ + K^{+} decay fraction is determined by the user defined decay table.

$$F_{Pythia}(B^{+} \rightarrow \mathrm{J}/\psi + \mathrm{K}^{+}) = 0.106$$

The fraction of $H_b \rightarrow$ J/ψ + X is simply 1 for Pythia since we force all B's from the b quark to decay to J/ψ. These numbers give the following correction factor.

$$C_{Norm} = 0.709 \pm 0.065$$

When we calculate the normalization using the $B^{\pm} \rightarrow$ J/ψ + K$^{\pm}$ peaks in data and Pythia we correct using C$_{Norm}$.

3 Correction to $b\bar{b}$ Production Mechanisms in Pythia

As discussed in Lannon [2], leading order calculations of $b\bar{b}$ production do not give results matching measurement, hence the need to include next to leading order (NLO) calculations. The production mechanisms included in the Pythia MC are:

- Flavor Creation (FC) - The leading order term where a $q\bar{q}$ or gg pair annihilates to create a $b\bar{b}$ pair. The angle between the b/bbar pair tends to be large in the lab frame.

- Flavor Excitation (FE) - NLO correction where one of the sea b quarks scatters off a quark or gluon. There are three bodies in the final state, allowing for smaller angles between the $b\bar{b}$ pair.

- Gluon Splitting (GS) - NLO correction where a scattered gluon creates a $b\bar{b}$ pair. As above the three bodies in the final state allow for smaller angles between the $b\bar{b}$ pair.

Appendix A contains a study of possible kinematic variables from the $b\bar{b}$ pair that could be used to tune the relative fractions of FC, FE and GS in Pythia. We find that the only variable that offers statistically significant seperation for the QCD processes is $\Delta\phi$, the azimuthal angle between the J/ψ and μ. Since B_c events tend to fall in the small $\Delta\phi$ region (hence a $\Delta\phi < \pi/2$ cut in the B_c analysis) it is especially important that we tune Pythia to give the proper $\Delta\phi$ distribution. To do this we use a data sample separate but similar to that used for the B_c analysis and fit the relative fractions of FC, FE and GS to the data, extracting scaling factors for the three production mechanisms: S_{FC}, S_{FE} and S_{GS}.

3.1 Unvertexed J/ψ+$\mu^{\pm}$ Sample

To adjust the relative fractions of the Pythia production mechanisms we use an unvertexed tri-muon data sample from 360 pb^{-1} of luminosity subject to the same cuts as those used in the B_c analysis [3] with the following differences. There is: no three muon vertex requirement, a pseudo-lifetime cut of 120μm on the two muon J/ψ vertex instead of 60μm cut on the three muon B_c vertex and no $\Delta\phi$ cut between the J/ψ and third muon. We define the pseudo-lifetime ct* as:

$$ct^* = \frac{L_{xy}(\mathrm{J}/\psi)\times \mathrm{M}(\mathrm{J}/\psi)}{P_t(\mathrm{J}/\psi)}$$

Figure 1 contains a fitted histogram of the J/ψ pseudo-lifetime at the J/ψ+track level. The fit function contains a prompt (gaussian), two positive lifetimes and a negative lifetime component. The fit gives a sigma of 32μm for the prompt component of the distribution. Our 120μm cut ensures that there is minimal prompt contamination in our sample.

Figure 2 contains the $\Delta\phi$ distribution of the unvertexed J/ψ+$\mu^{\pm}$ data. We expect this distribution to consist of decay-in-flight/punch-through, fake J/ψ and B_c events in addition to $b\bar{b}$ events. These backgrounds to the $b\bar{b}$ signal will be discussed in the following sections. Figure 3 contains the $\Delta\phi$ for the Pythia sample which is pure $b\bar{b}$.

The drop off at large $\Delta\phi$ in the data (Figure 2) is of interest as it would potentially affect the results of our fit. Figure 3 showing the $\Delta\phi$ from the Pythia sample does not exhibit the same behavior at large $\Delta\phi$ even though we expect the data to be dominated by $b\bar{b}$ processes at large $\Delta\phi$. Currently we are unable to explain the drop off in the data at large $\Delta\phi$, therefore we throw out events with $\Delta\phi$>2.98. We also throw out events at small $\Delta\phi$ (<0.079) because the isolation cut from the B_c analysis

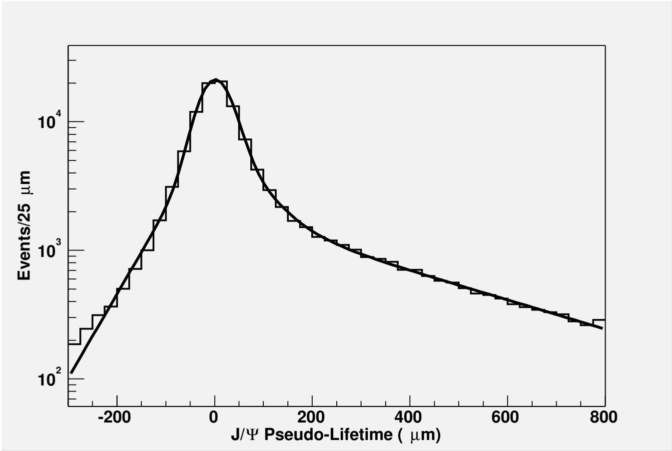

Figure 1: Fitted J/ψ pseudo-lifetime distribution.

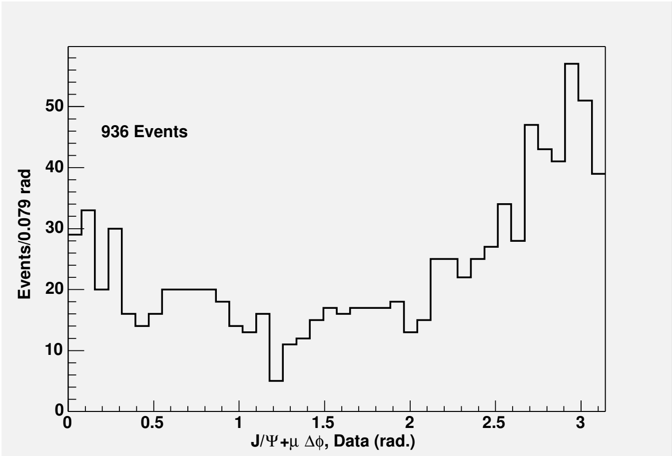

Figure 2: $\Delta\phi$ distribution for the unvertexed J/ψ+$\mu^{\pm}$ data sample.

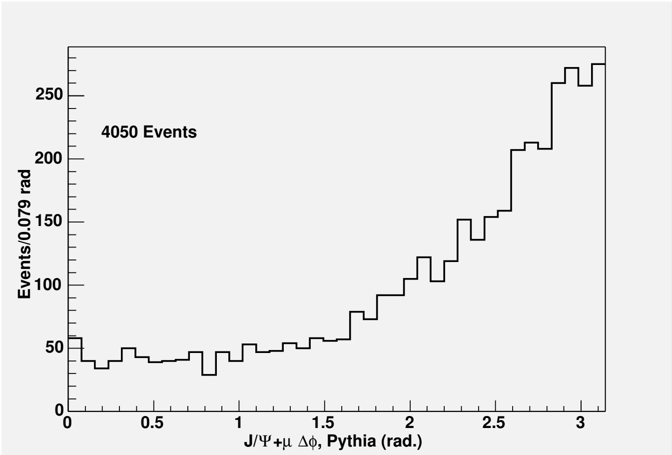

Figure 3: $\Delta\phi$ distribution for the unvertexed J/ψ+$\mu^{\pm}$ Pythia sample.

leads to poor agreement with fit results at small $\Delta\phi$, particularly for the B_c fit, as will be discussed in section 3.5. In addition we see a possible drop off at small $\Delta\phi$ in the data (Figure 2) which we are not sure that our Monte Carlos can properly model.

3.2 Production Mechanism Components of Pythia Sample

Before we can fit the relative fractions of the FC, FE and GS production mechanisms to data, we must split the Pythia sample up into the three production mechanisms and fit template functions to each distribution seperately. Figure 4 shows J/ψ+$\mu^{\pm}$ $\Delta\phi$ distributions for each of the production mechanisms as well as the resulting fitted templates. Each fit is an unbinned log-likelihood with the likelihood functions $\prod_i F_{FC}(\Delta\phi_i)$, $\prod_i F_{FE}(\Delta\phi_i)$, and $\prod_i F_{GS}(\Delta\phi_i)$ where

$$F_{FC}(\Delta\phi_i) = P_{1FC}C_{FC}e^{P_{0FC}\Delta\phi_i}$$

$$F_{FE}(\Delta\phi_i) = C_{FE}(P_{0FE}(\Delta\phi_i)^3 + P_{1FE}(\Delta\phi_i)^2 + P_{2FE}\Delta\phi_i + P_{3FE})$$

$$F_{GS}(\Delta\phi_i) = C_{GS}(P_{0GS}(\Delta\phi_i)^2 + P_{1GS}\Delta\phi_i + P_{2GS}).$$

The P factors are the parameters for each fit and the C factors are normalization factors that depend on the paramaters. The C factors depend on the parameters because it is important that the functions have a fixed integral so the fitter does not simply increase the total area under the function in order to increase the likelihood.

3.3 Decay-in-Flight/Punch-Through (DIF/PT) Background

One source of background to $b\bar{b}$ are events where a J/ψ forms a vertex with a hadron which proceeds to either decay in flight to a μ or punch through the calorimetry to the muon chamber. To study the shape and number of these events we begin with an unvertexed J/ψ+track data set where the third track has the same requirements as in the J/ψ+$\mu^{\pm}$ data except for the muon requirements. The $\Delta\phi$ distribution for this can be seen in Figure 5. By determining the relative fraction of kaons, pions and protons as third tracks in this sample and applying calculated DIF/PT rates we can determine the DIF/PT $\Delta\phi$ distribution.

To calculate the relative K/P/π fractions in the J/ψ+track data we use dE/dx measurements. The data is broken up into eight momentum ranges: 3.0-3.5GeV/c, 3.5-4.0GeV/c, 4.0-4.5GeV/c, 4.5-5.0GeV/c, 5.0-6.0GeV/c, 6.0-7.0GeV/c, 7.0-8.0GeV/c and >8GeV/c. For each bin we fit three gaussians, representing the kaon, proton and π fractions, to a dE/dx pull distribution with a pion hypothesis calculated using the following formula:

$$\left(\frac{dE}{dx}\right)_{Pull} = \frac{dE/dx_{\pi} - <dE/dx>_{\pi}}{\sigma_{\pi}}$$

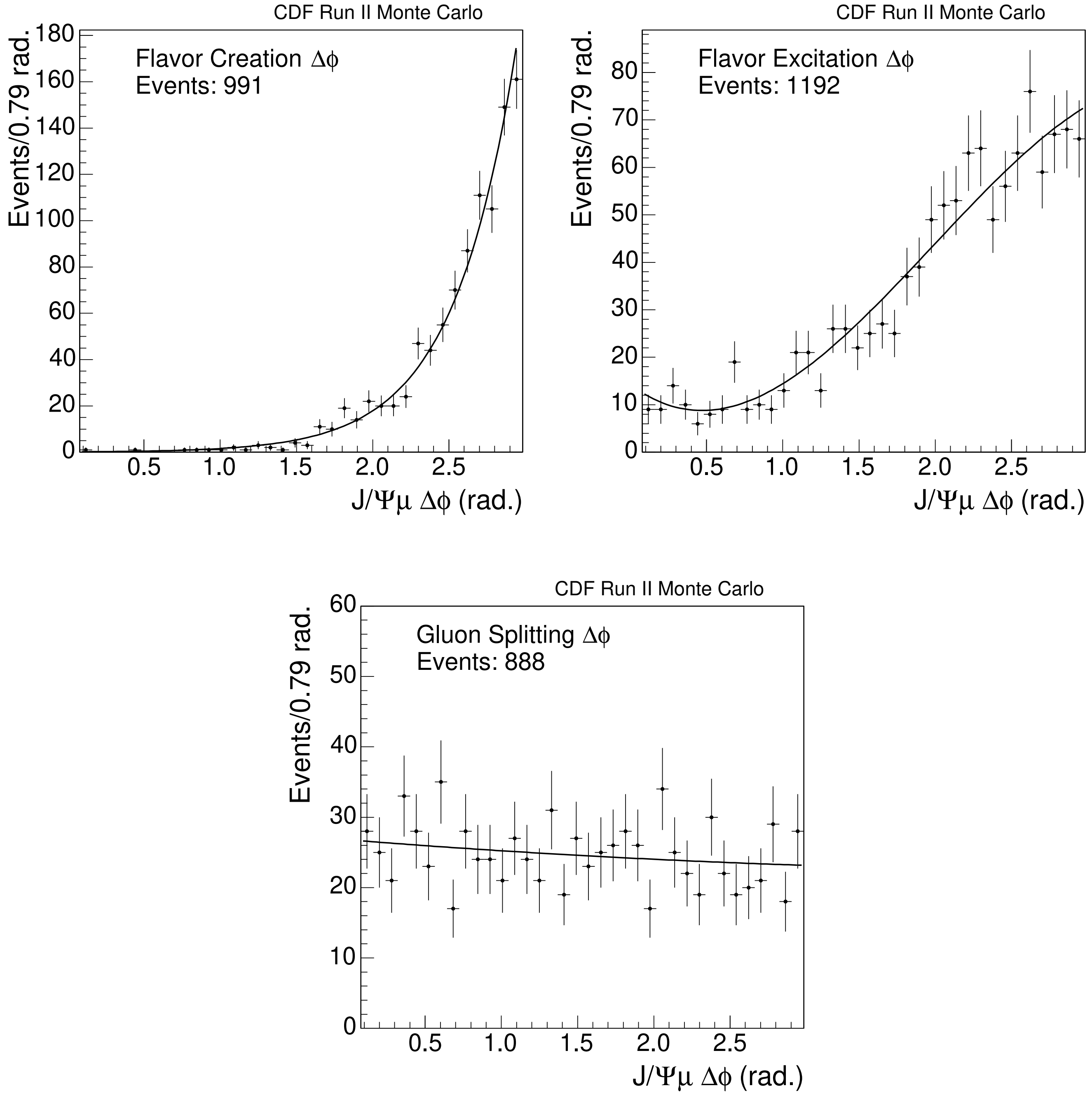

Figure 4: Top left: Pythia FC J/ψ+$\mu^{\pm}$ $\Delta\phi$ with results of unbinned log-likelihood fit. Top right: Pythia FE J/ψ+$\mu^{\pm}$ $\Delta\phi$ with results of unbinned log-likelihood fit. Bottom: Pythia GS J/ψ+$\mu^{\pm}$ $\Delta\phi$ with results of unbinned log-likelihood fit.

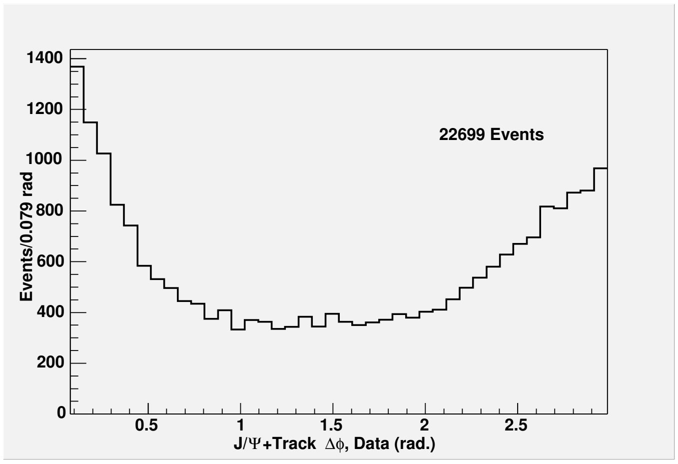

Figure 5: J/ψ+track $\Delta\phi$ distribution.

The size of the proton contribution is fixed relative to the kaons by the rates given in the PDG [1] for B hadrons to decay to protons and kaons respectively:

$$\frac{F(H_b->P^{\pm})}{F(H_b->K^{\pm})} = 0.177 \pm 0.021$$

The results of the fits can be seen in Figure 6 and Figure 7. The resulting hadron fractions are in Table 1.

$Momentum$	F_π	$F_{(K+P)}$
$3.0-3.5$	0.661 ± 0.013	0.279 ± 0.066
$3.5-4.0$	0.629 ± 0.013	0.305 ± 0.063
$4.0-4.5$	0.644 ± 0.017	0.293 ± 0.065
$4.5-5.0$	0.646 ± 0.021	0.291 ± 0.066
$5.0-6.0$	0.612 ± 0.019	0.319 ± 0.062
$6.0-7.0$	0.640 ± 0.030	0.296 ± 0.067
$7.0-8.0$	0.560 ± 0.045	0.362 ± 0.066
> 8.0	0.660 ± 0.036	0.280 ± 0.071

Table 1: π fractions in the J/ψ+track sample.

Once we have identified the probability that a track is a K, P or π we can apply the DIF/PT rates to determine a DIF/PT probablilty for each individual third track. DIF/PT rates are determined in CDF Note 6956 [3]. For kaons and pions the DIF/PT rates are calculated using $D^0 \rightarrow \pi + K$ where the π and K are tagged by reconstructing D^*. Results are presented in Table 2. For protons an upper limit of 3.4×10^{-4} is placed on the PT rate by looking at lambda decays, leading to the conclusion that protons are not a significant source of punch through.

After applying the DIF/PT rates and π/K/P fractions to the third tracks in the J/ψ+tracks sample we are left with the $\Delta\phi$ distribution shown in Figure 8 which

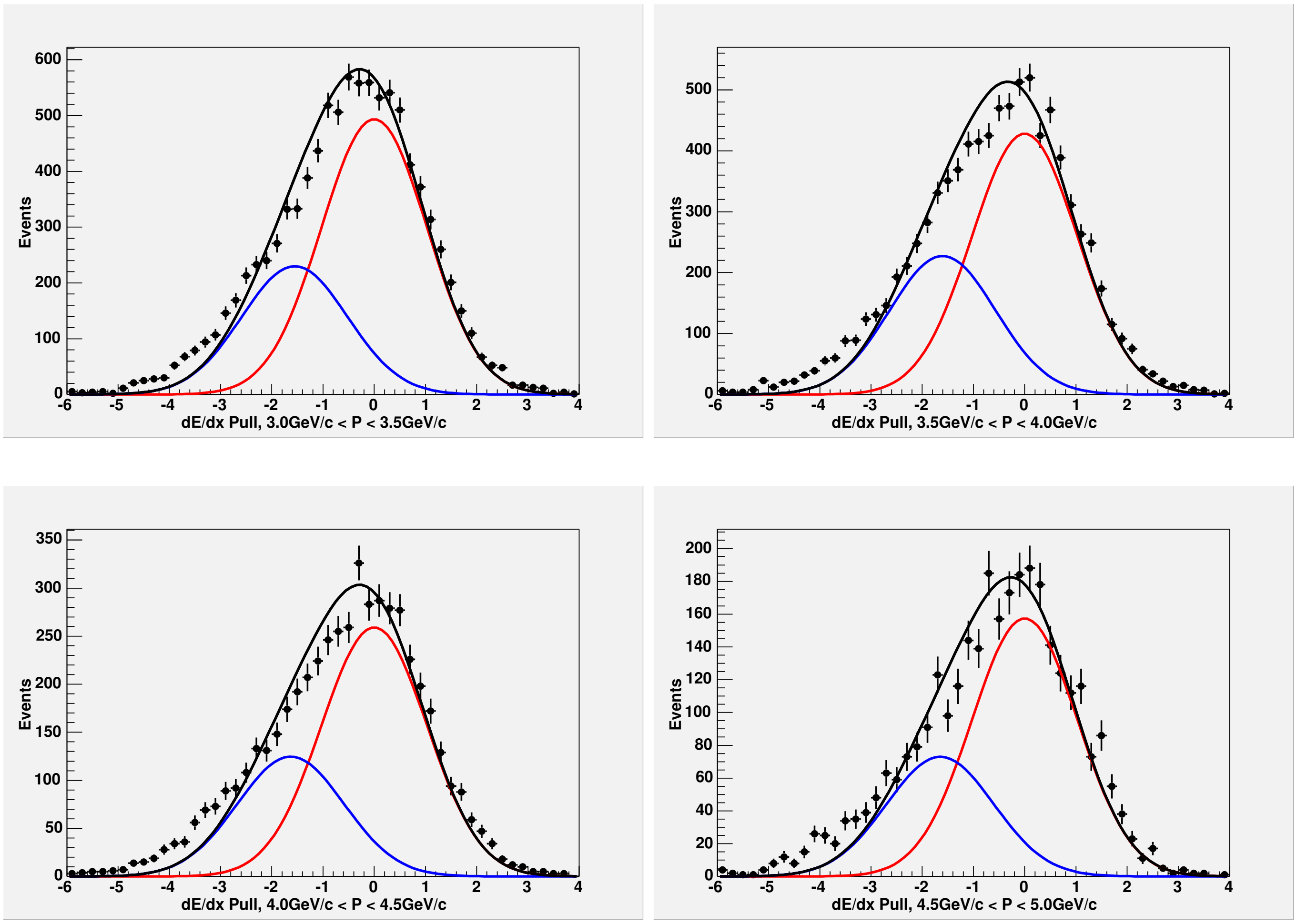

Figure 6: dE/dx pull fits for tracks with 3.0GeV/c<P<5.0GeV/c. Red is the π contribution, blue the K+P. Top left: Tracks with momentum 3.0-3.5GeV/c. Top right: Tracks with momentum 3.5-4.0GeV/c. Bottom left: Tracks with momentum 4.0-4.5GeV/c. Bottom right: Tracks with momentum 4.5-5.0GeV/c.

P_t	$3-4$ GeV/c	$4-5$ GeV/c	$5-7$ GeV/c	>7 GeV/c
π	0.00246 ± 0.00026	0.00307 ± 0.00038	0.00251 ± 0.00041	0.00233 ± 0.00079
K^+	0.00559 ± 0.00059	0.00663 ± 0.00084	0.00802 ± 0.00110	0.0116 ± 0.00250
K^-	0.00438 ± 0.00056	0.00487 ± 0.00076	0.00382 ± 0.00078	0.00799 ± 0.00216

Table 2: Pion and kaon DIF/PT rates.

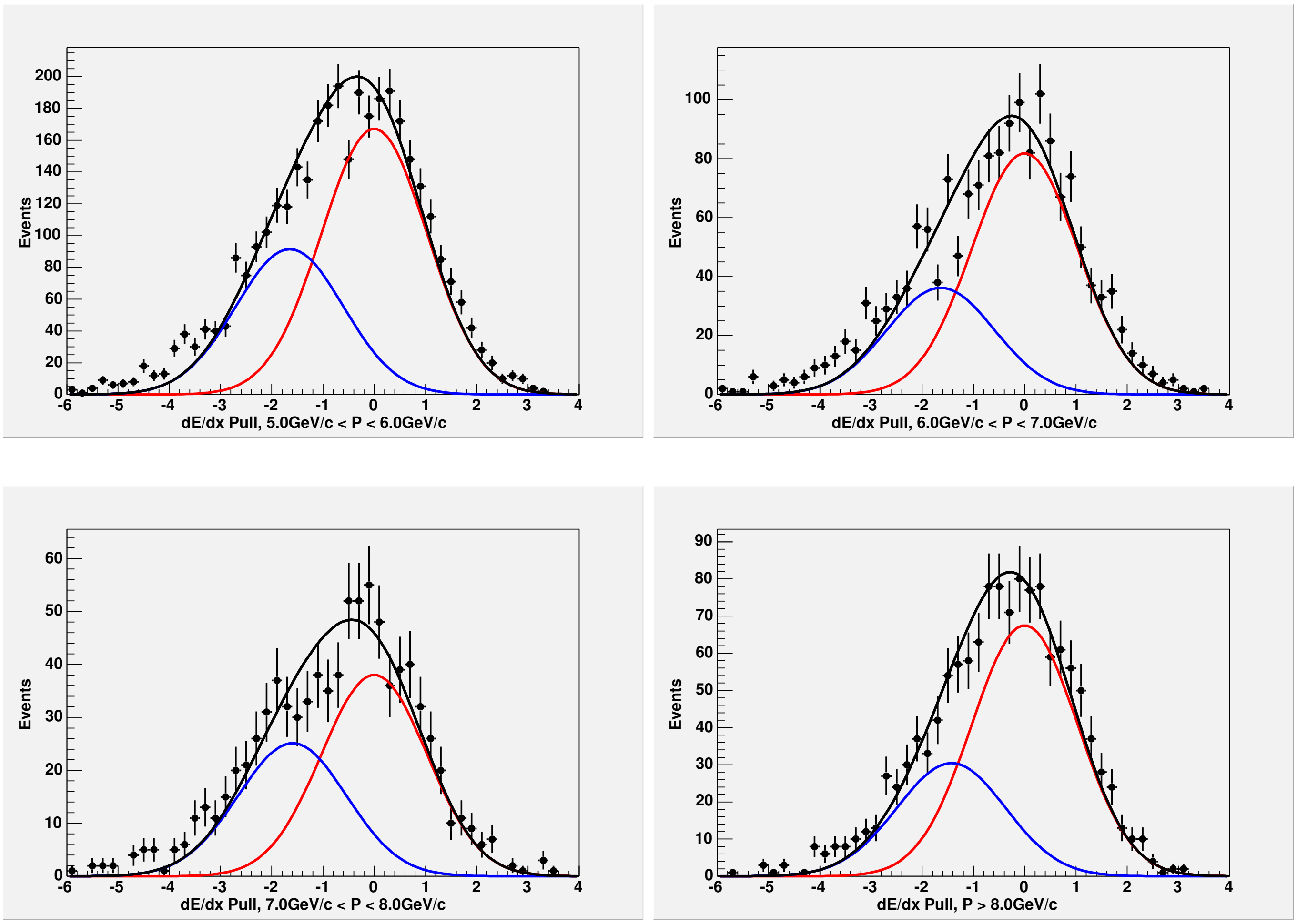

Figure 7: dE/dx pull fits for tracks with P>5.0GeV/c. Red is the π contribution, blue the K+P. Top left: Tracks with momentum 5.0-6.0GeV/c. Top right: Tracks with momentum 6.0-7.0GeV/c. Bottom left: Tracks with momentum 7.0-8.0GeV/c. Bottom right: Tracks with momentum >8GeV/c.

also contains the results of an unbinned log-likelihood fit to the distribution. The likelihood function used is $\prod_i D_i F_{DP}(\Delta\phi_i)$.

$$F_{DP}(\Delta\phi_i) = C_{DP}(P_0(\Delta\phi_i)^4 + P_1(\Delta\phi_i)^3 + P_2(\Delta\phi_i)^2 + P_3\Delta\phi_i + P_4)$$

D_i is the DIF/PT probability for each third track, P_0-P_4 are the fit parameters and C_{DP} is a normalization factor that depends on the fit parameters. The total predicted DIF/PT background is 74.9±2.9 events. The error is calculated using the errors from the determination of the DIF/PT rates and the π/K/P fractions as well as the statistical error on the J/Ψ+track sample.

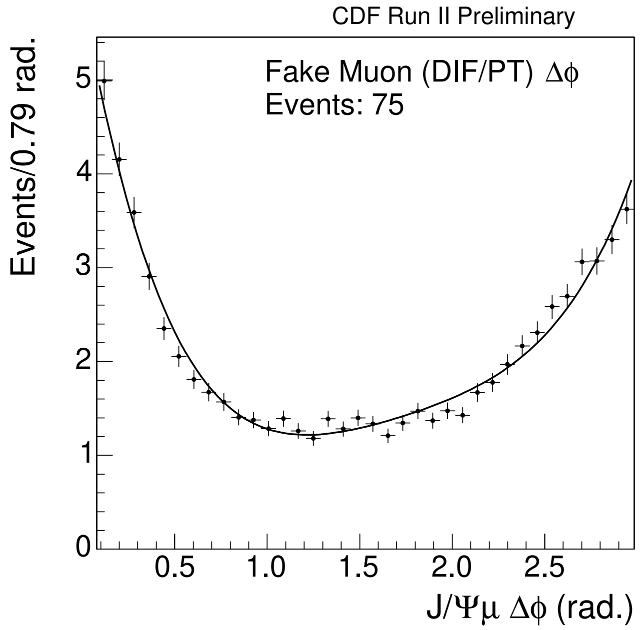

Figure 8: Predicted J/ψ+$\mu^\pm$ $\Delta\phi$ for DIF/PT events

3.4 Fake J/ψ Background

Another background present in the data sample, but not Pythia, are fake J/ψ events where a third μ is matched with two μ's that fake a J/ψ. To determine the size and shape of this sample for the fit, we look at the sidebands of the J/ψ mass peak from our unvertexed J/ψ+track data sample, as shown in Figure 9. Using the highlighted sideband regions (and normalizing by 0.5) we select events that pass all of the unvertexed J/ψ+$\mu^\pm$ cuts except for the J/ψ mass cut. The resulting events give an estimate of the size and shape of the fake J/ψ background under the J/ψ mass peak.

Figure 10 shows the J/ψ+$\mu^\pm$ $\Delta\phi$ for fake J/ψ events as well as the fit results. The fitting method is unbinned log-likelihood with the likelihood function $\prod_i F_{FJ}(\Delta\phi_i)$.

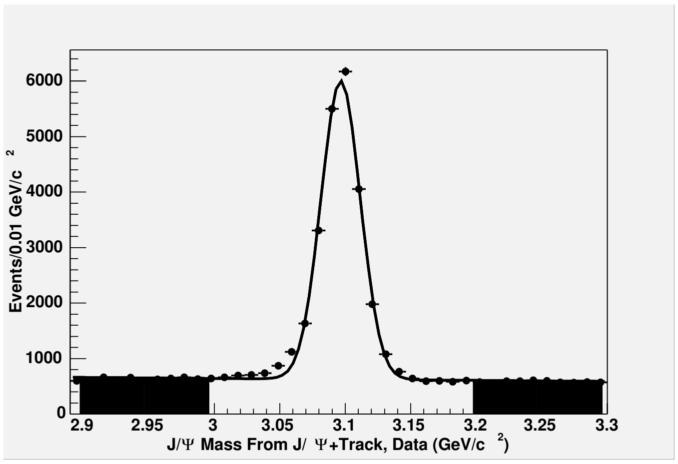

Figure 9: J/ψ for J/ψ+track events. The shaded sideband regions are used to determine the size and shape of the fake J/ψ contribution to the J/ψ+$\mu^{\pm}$ $\Delta\phi$ distribution in data.

$$F_{FJ}(\Delta\phi_i) = C_{FJ}(P_0(\Delta\phi_i)^3 + P_1(\Delta\phi_i)^2 + P_2\Delta\phi_i + P_3)$$

P_0 through P_3 are the parameters of the fit, while C_{FJ} is the normalization which also depends on the fit parameters. The total fake J/ψ background is 154.0±12.4(stat.)±7.8(syst.) events. The systematic error is determined using the uncertainty in the J/ψ signal from the fit in Figure 9.

3.5 Fake J/ψ, DIF/PT Double Counting

It is possible for an event to be both a fake J/ψ and to have a third track that is identified as a muon because it decays in flight or punches through. To quantify this double counting we look at the fake J/ψ+track sample and apply our DIF/PT rates to the third tracks in this sample. The resulting distribution is shown below and fitted with the likelihood function $\prod_i D_i F_{DF}(\Delta\phi_i)$.

$$F_{DF}(\Delta\phi_i) = C_{DF}(P_0(\Delta\phi_i)^4 + P_1(\Delta\phi_i)^3 + P_2(\Delta\phi_i)^2 + P_3\Delta\phi_i + P_4)$$

P_0 through P_4 are the parameters of the fit, while C_{DF} is the normalization which also depends on the fit parameters. The total fake J/ψ + DIF/PT background is 17.4±1.0 events. When we fit the total $\Delta\phi$ distribution this contribution is subracted out so as to avoid double counting.

3.6 B_c Background

The final background contribution to the J/ψ+$\mu^{\pm}$ $\Delta\phi$ are B_c events. We are unable to determine the size of the the B_c contribution independently of the B_c analysis, but we can determine the shape using a MC sample generated with BGenerator. The

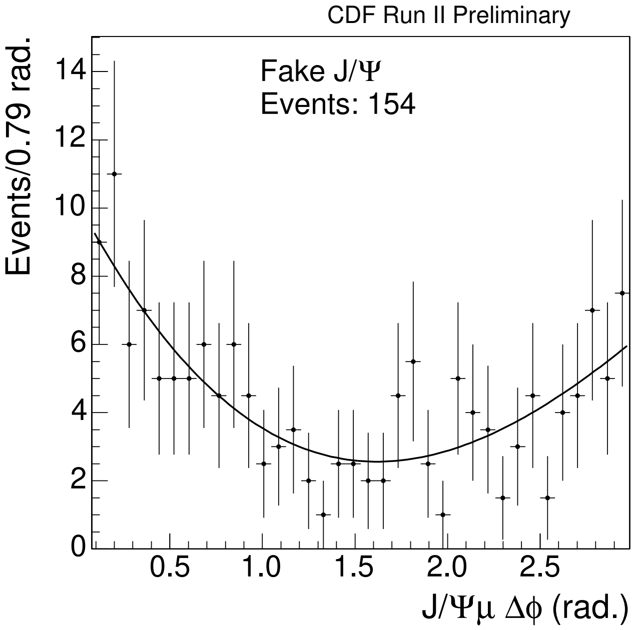

Figure 10: Fake J/ψ+$\mu^{\pm}$ $\Delta\phi$ with results of unbinned log-likelihood fit

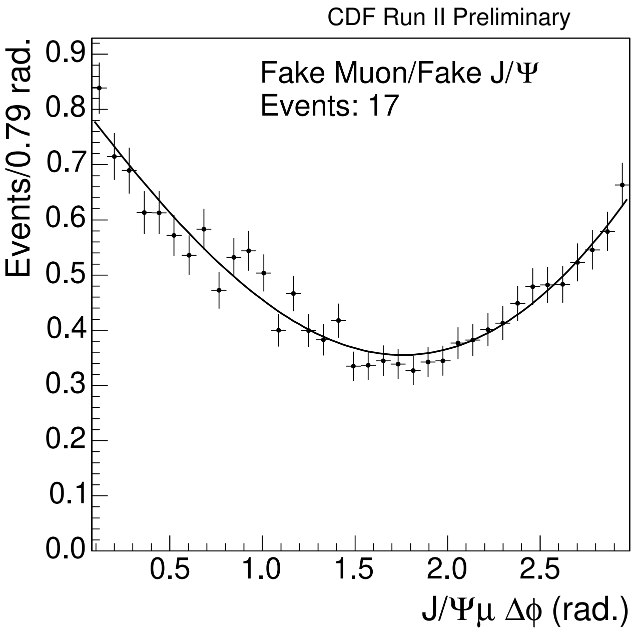

Figure 11: Fake J/ψ + DIF/PT $\Delta\phi$ with results of unbinned log-likelihood fit

resulting distribution, shown in Figure 12, is fitted using an unbinned log-likelihood fit with the function $\prod_i F_{BC}(\Delta\phi_i)$

$$F_{BC} = C_{BC} e^{-\frac{1}{2}\frac{(\Delta\phi_i - P_1)^2}{P_0^2}}$$

P_0 and P_1 are the fit parameters and C_{BC} gives the proper normalization and depends on the parameters.

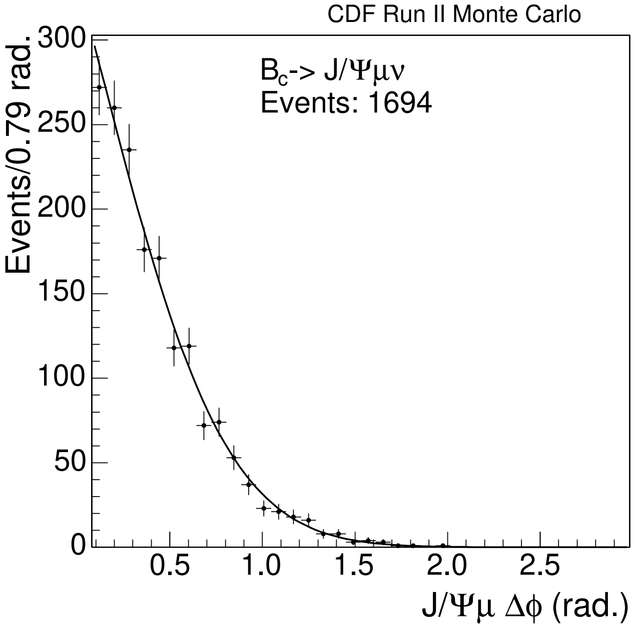

Figure 12: B_c J/ψ+$\mu^\pm$ $\Delta\phi$ from BGenerator with results of unbinned log-likelihood fit.

As mentioned in section 3.1 we have dropped events with $\Delta\phi$<0.079 because of the poor agreement between the fit and the MC events at small angle. This can be seen in the first bin of Figure 13. The poor agreement is caused by the isolation cut from the B_c analysis, which is more likely to throw out events where the J/ψ and $\mu^\pm$ are in the same direction, causing the MC data to fall off at small $\Delta\phi$. Since it is difficult to model this effect in the fit function and we are not sure that the MC sample is affected the same as data, we throw out these events.

3.7 J/ψ+$\mu^\pm$ $\Delta\phi$ Fitting Procedure

Having determined template functions for the background contributions and productions mechanisms, we are now able to do a fit to the full J/ψ+$\mu^\pm$ $\Delta\phi$ in data where we allow the relative fractions of production mechanisms to float. The log likelihood function used for the fit is:

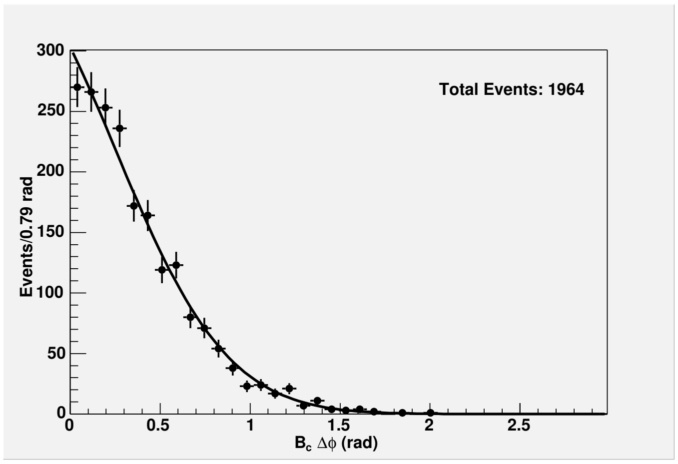

Figure 13: B_c J/ψ+$\mu^{\pm}$ $\Delta\phi$ from BGenerator small angle included.

$$-2[\sum_i ln(\frac{P_0}{P_5+P_6+P_7}(P_5F_{FC}+P_6F_{FE}+P_7F_{GS})+P_1F_{DP}+P_2F_{FJ}$$

$$+P_3F_{BC}-P_4F_{DF})]-2ln(N_{TOT})-2ln(P_0+P_1+P_2+P_3-P_4)+\frac{(P_2N_{TOT}-<N_{FJ}>)^2}{\sigma^2_{FJ}}$$

$$+\frac{(P_1N_{TOT}-<N_{DP}>)^2}{\sigma^2_{DP}}+\frac{(P_4N_{TOT}-<N_{DF}>)^2}{\sigma^2_{DF}}+XC^{-1}X+\frac{(N_{b\bar{b}}-<N_{b\bar{b}}>)^2}{\sigma^2_{b\bar{b}}}$$

The F functions are the previously fitted templates. The P_0, P_1, P_2, P_3 and P_4 parameters give the fractions of our componenets and P_1, P_2 and P_4 are constrained by the predicted numbers $<N_{DP}>$, $<N_{FJ}>$ and $<N_{DF}>$. The scale factors for the production mechanisms are given by:

$$S_{FC}=\frac{P_5}{P_5+P_6+P_7}\frac{1}{F_{FC}}$$

$$S_{FE}=\frac{P_6}{P_5+P_6+P_7}\frac{1}{F_{FE}}$$

$$S_{GS}=\frac{P_7}{P_5+P_6+P_7}\frac{1}{F_{GS}}$$

Where F_{FC}, F_{FE} and F_{GS} are the default relative fractions of the production mechanisms in Pythia. X is a vector of the the parameters from the previous fits of the F functions which is constrained by the covariance matrix from those fits given by C.

The constraint on $N_{b\bar{b}}$ comes from the fact that we require the normalization of the Pythia sample to data to give the correct result (within errors) as we adjust the scale factors S_{FC}, S_{FE} and S_{GS}. We can write this requirement as:

$$P_0N_{TOT}=\frac{(S_{FC}N_{FC}+S_{FE}N_{FE}+S_{GS}N_{GS})N_{data}(B^{\pm})}{(S_{FC}N_{FC}(B^+)+S_{FE}N_{FE}(B^+)+S_{GS}N_{GS}(B^+))C_{Norm}}$$

The left side gives $N_{b\bar{b}}$ and the right $<N_{b\bar{b}}>$. $N_X(B^+)$ are the number of $B^{\pm}\rightarrow$ J/ψ+ $K^{\pm}$ for data and the three production mechanisms which can be seen in Figure 14. $\sigma_{b\bar{b}}$, determined by the errors on all of the measured values in the previous equation, is 71.5.

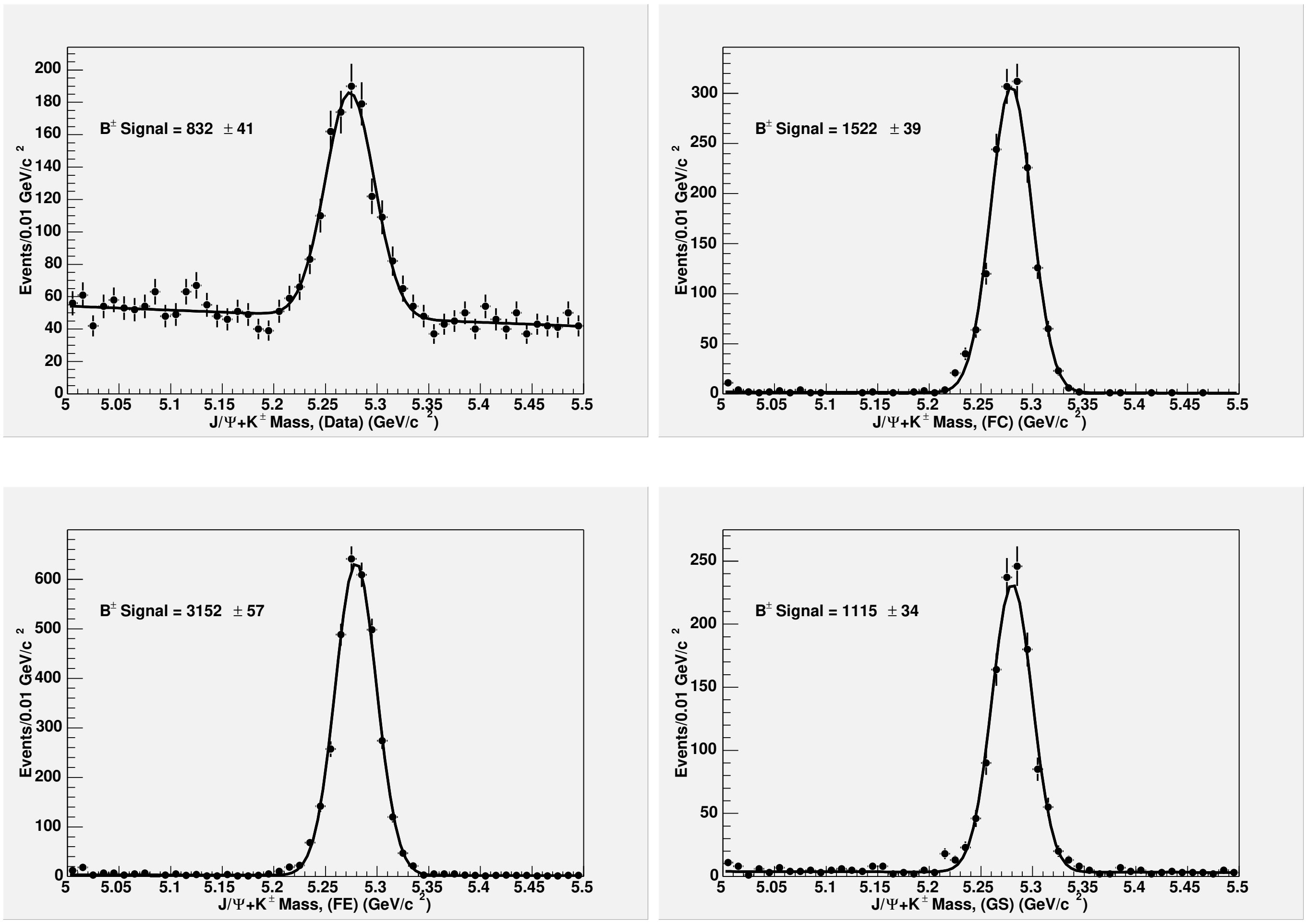

Figure 14: $B^{\pm} \to \mathrm{J}/\psi + \mathrm{K}^{\pm}$ fits for data and Pythia production mechanisms. Top left: Data. Top right: Flavor Creation. Bottom left: Flavor Excitation. Bottom right: Gluon Splitting.

3.8 $J/\psi+\mu^{\pm}$ $\Delta\phi$ Fit Results

The results of the fit can be seen in Figure 15 and the fit values for the parameters can be seen in Table 3. The resulting scale factors from the log likelihood fit are:

$$S_{FC} = 0.902 \pm 0.205$$
$$S_{FE} = 0.810 \pm 0.365$$
$$S_{GS} = 1.36 \pm 0.39$$

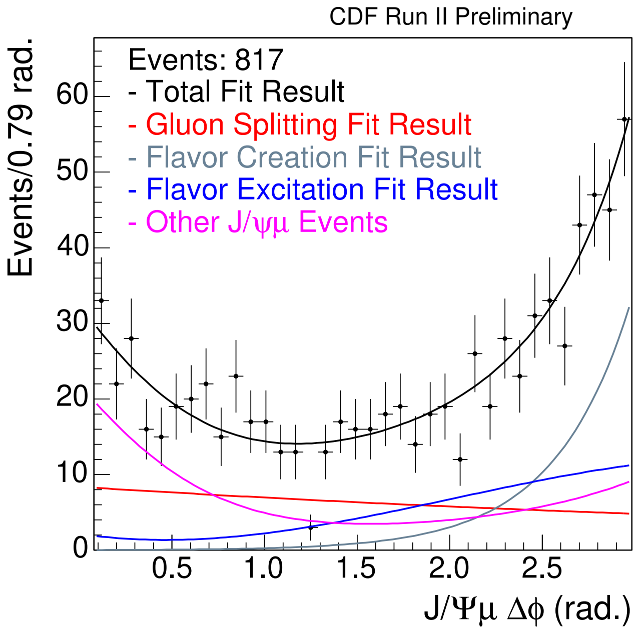

Figure 15: $J/\psi+\mu^{\pm}$ $\Delta\phi$ data distribution and fit results. Colored curves are fitted $b\bar{b}$ contributions.

Parameter Number	Description	Value	Error
P_0	$b\bar{b}$ fraction	0.713	0.052
P_1	DIF/PT fraction	0.091	0.011
P_2	Fake J/ψ fraction	0.185	0.026
P_3	B_c fraction	0.043	0.039
P_4	Double Counting fraction	0.022	0.005
P_5	FC coefficient	0.291	0.071
P_6	FE coefficient	0.315	0.143
P_7	GS coefficient	0.395	0.117

Table 3: Parameters from the $J/\psi+\mu^{\pm}$ $\Delta\phi$ fit.

3.9 Verification of Fit Results

To verify the scale factors extracted from the fit, we look at the $J/\psi+\mu^{\pm}$ mass distribution at masses larger than 6.0GeV/c^2. According to nonrelativistic potential models the B_c mass is calculated to be 6.194-6.292GeV/c^2 [4]. With this mass range a negligible number of B_c $J/\psi+\mu^{\pm}$ pairs will have mass greater than 6.0GeV/c^2 and this high mass region will be dominated by our B_c backgrounds. We compare the mass distribution for data with a distribution consisting of the DIF/PT and fake J/ψ predictions as well as the scaled Pythia productions mechanisms for both vertexed and unvertexed events. The results are shown in Figure 16. For unvertexed data we find 702 events >6.0GeV/c^2 compared to 725 predicted events, for vertexed data 59 events >6.0GeV/c^2 compared to 63 predicted.

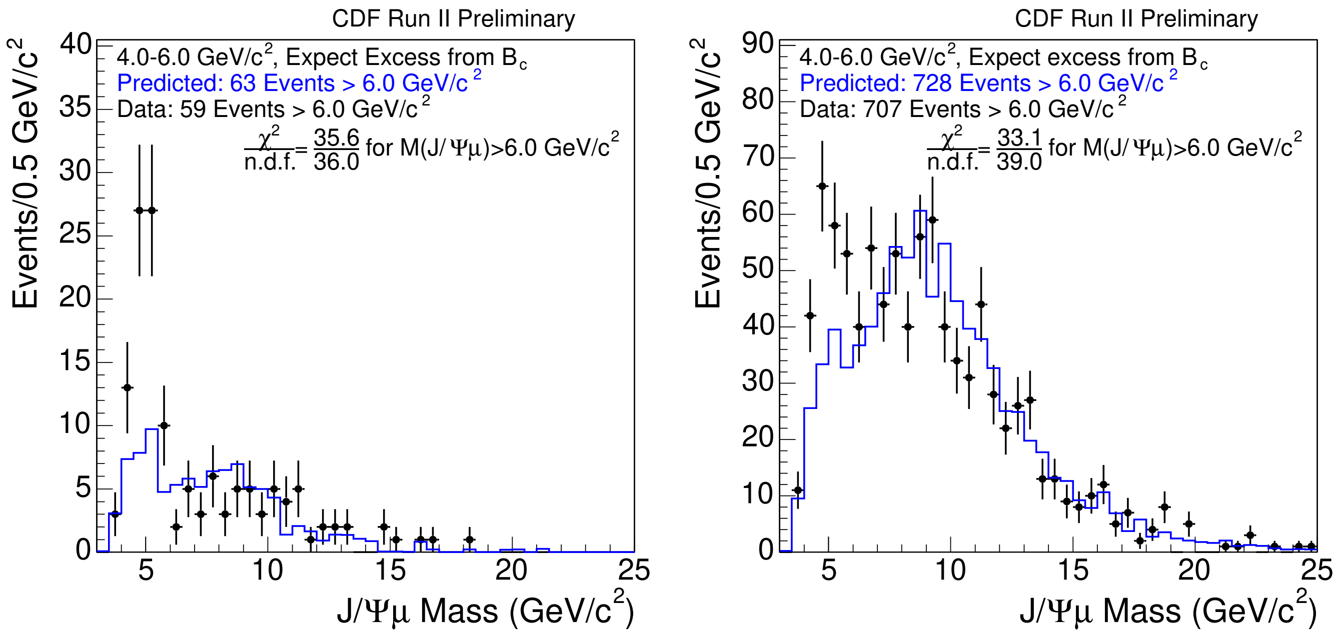

Figure 16: $J/\psi+\mu^{\pm}$ mass distributions for vertexed and unvertexed data. Black is data, blue is Pythia scaled using fit results plus predicted DIF/PT and fake J/ψ for unvertexed data. Left: Vertexed data. Right: Unvertexed data.

We can also look at the $J/\psi+\mu^{\pm}$ mass distribution for $\Delta\phi > \frac{\pi}{2}$. As we saw in Figure 12 this region contains no B_c events and is populated purely by the backgrounds to B_c. Results are shown for vertexed and unvertexed data in Figure 17. For vertexed data we predict 57 events versus 54 measured, for vertexed data we predict 618 events versus 572 measured.

As a final check on our results we calculate the fraction of $b\bar{b}$ events with $\Delta\phi<\pi/2$ and compare with the results in CDF Note 7253 [5]. This calculation is done by subtracting the backgrounds to $b\bar{b}$ (DIF/PT, fake J/ψ and B_c) as determined by the fit and then calculating the forward fraction of $J/\psi+\mu^{\pm}$ events. Our value of

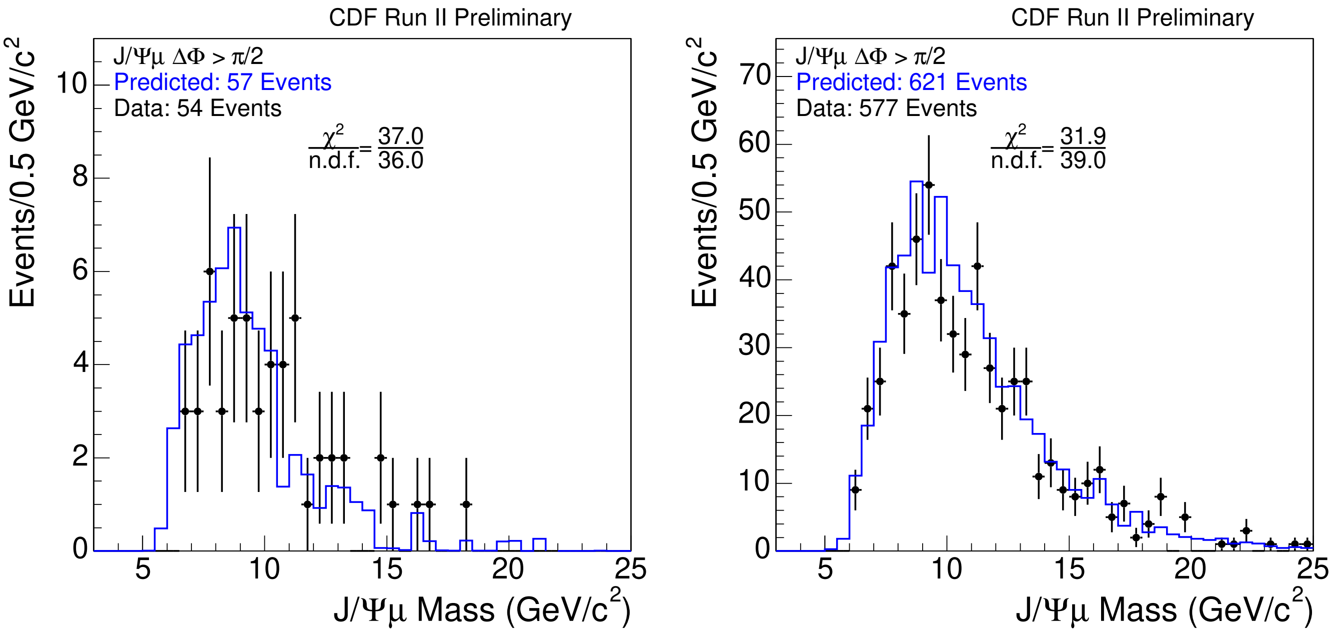

Figure 17: J/ψ+$\mu^{\pm}$ mass distributions for vertexed and unvertexed data with $\Delta\phi{>}\pi/2$. Black is data, blue is Pythia scaled using fit results plus predicted DIF/PT and fake J/ψ for unvertexed data. Left: Vertexed data. Right: Unvertexed data.

0.278±0.048 is in good agreement with previous results.

4 $b\bar{b}$ Background Calculation

Having calculated the correction factor for the Pythia B$^+$ production cross section and $B^+ \rightarrow$ J/ψ + K$^+$ decay fraction, and the scale factors for the Pythia production mechanisms we are able to calculate the $b\bar{b}$ background for vertexed J/ψ+$\mu^{\pm}$ events. For this calculation we use the data set used in CDF Note 6956 [3] which contains 360 pb^{-1} of data. The formula for calculating the $b\bar{b}$ background is given below.

$$N_{b\bar{b}} = (N_{FC}S_{FC} + N_{FE}S_{FE} + N_{GS}S_{GS})\frac{N_{Data}(B^{\pm})}{(N_{FC}(B^{\pm})S_{FC}+N_{FE}(B^{\pm})S_{FE}+N_{GS}(B^{\pm})S_{GS})C_{Norm}}$$

We find the number of events for each production mechanism by applying B_c analysis cuts to the Pythia sample and counting the number of events left for each production mechanism.

$$N_{FC} = 1$$
$$N_{FE} = 17$$
$$N_{GS} = 41$$

We fit the $B^{\pm} \rightarrow$ J/ψ + K$^{\pm}$ peaks for data and the Pythia production mechanisms (Figure 18) for use in normalization, giving the following numbers.

$$N_{Data}(B^{\pm}) = 755 \pm 30$$
$$N_{FC}(B^{\pm}) = 1293 \pm 36$$
$$N_{FE}(B^{\pm}) = 2688 \pm 52$$
$$N_{GS}(B^{\pm}) = 962 \pm 31$$

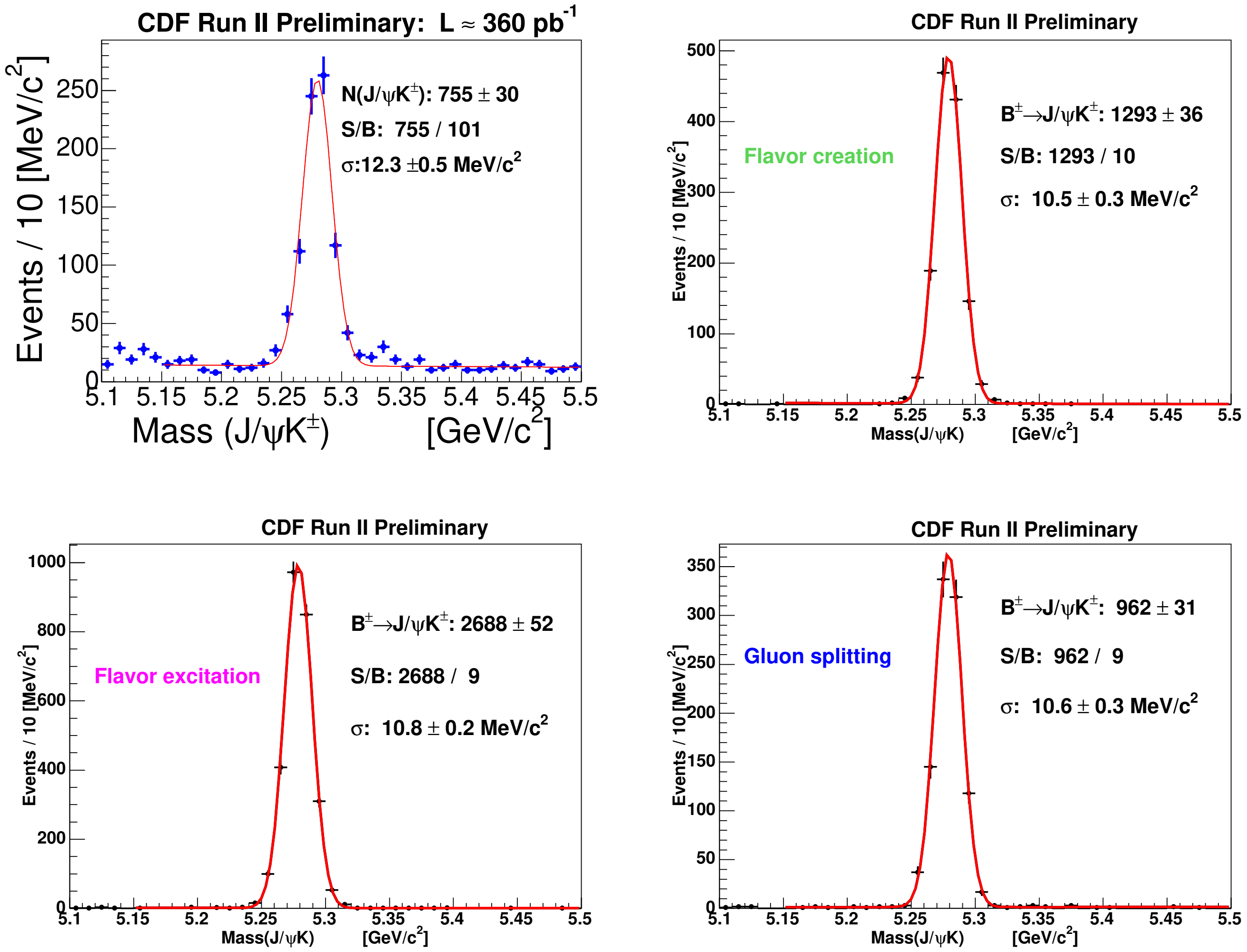

Figure 18: Vertexed $B^{\pm} \to \mathrm{J}/\psi+\mathrm{K}^{\pm}$ fits for data and Pythia production mechanisms. Top left: Data. Top right: Flavor Creation. Bottom left: Flavor Excitation. Bottom right: Gluon Splitting.

The calculated $b\bar{b}$ background is: 16.1 ± 2.1(stat.)± 4.3(syst.). Here the statistical error comes from the 59 $b\bar{b}$ events that make B_c candidates and the systematic error comes from the propagation of errors from the scale factor fit and other factors that we use to normalize Pythia to data. We calculate an additional component of the systematic error due to our fitting procedure in the following section.

5 Systematic Errors From Fitting Procedure

We look for sources of systematic error in our scale factor fitting procedure and propagate these errors forward through a calculation of the $b\bar{b}$ background to determine a systematic for the $b\bar{b}$. The possible sources of error are: fitting program bias, the J/Ψ pseudo-lifetime cut, the $\frac{\mathrm{J}/\psi+\mu}{\mathrm{J}/\psi+\mathrm{K}}$ rate in Monte Carlo, the B_c $\Delta\phi$ shape and the possiblilty of an additional unknown background.

5.1 Fitting Program Bias

To check for a systematic error in our fitting program we generate 200 Monte Carlos of J/ψ+$\mu^{\pm}$ $\Delta\phi$ events using the templates that we have determined from data and Pythia. For these Monte Carlos we use our previously determined scale factors as input to the generation of the Monte Carlos. We then run our fitting program on each of the Monte Carlos and extract a value for the scale factors. We find the following average values for the scale factors:

$$S_{FC} = 0.890$$
$$S_{FE} = 0.868$$
$$S_{GS} = 1.30$$

These scale factors give a $b\bar{b}$ prediction of 15.5 which differs from the expected value of 16.1. We assign the difference of 0.6 as a systematic error.

5.2 J/Ψ Pseudo-lifetime Cut

In the B_c analysis we apply a pseudo-lifetime cut of 60μm to the J/ψ+μ candidates. For this analysis we have increased the pseudo-lifetime requirement to 120μm and applied it to the J/ψ so as to remove any prompt J/ψ component. To study the possible effect of this requirement and the possible presence of residual prompt J/ψ we decrease the requirement to 60μm and increase to 180μm, refitting with the following results:

Cut	S_{FC}	S_{FE}	S_{GS}	bb
60μm	0.810	0.955	1.28	15.3
180μm	0.781	0.815	1.48	17.3

These scale factors give a maximum deviation of 1.2 events from the nominal value, which we assign as the systematic error for this effect.

5.3 $\frac{\mathrm{J}/\psi+\mu}{\mathrm{J}/\psi+\mathrm{K}}$ Rate

Since we fit the scale factors to give the correct $\frac{\mathrm{J}/\psi+\mu}{\mathrm{J}/\psi+\mathrm{K}}$ ratio (which is used when normalizing to data) in addition to adjusting for the proper $\Delta\phi$ distribution, we check to see how adjusting the $\frac{J/\psi+\mu}{J/\psi+K}$ in the Monte Carlo affects the scale factor fit and the $b\bar{b}$ prediction. We adjust the rate of $J/\psi + \mu$ relative to $J/\psi + K$ by $\pm 10\%$ and see the following results:

Adjustment	S_{FC}	S_{FE}	S_{GS}	bb
+10%	0.859	0.928	1.25	16.6
−10%	0.959	0.652	1.51	16.0

We use the maximum difference from the calculated $b\bar{b}$ prediction to give a systematic of 0.5 events.

5.4 B_c $\Delta\phi$ Shape

Since the input spectrum for simulating B_c events is not well known, there is some uncertainty concerning the shape of the $J/\psi+\mu^{\pm}$ $\Delta\phi$ distribution from B_c events. To test the effect of this uncertainty we adjust the width of our B_c template by $\pm 10\%$ and extract new scale factors and $b\bar{b}$ predictions:

Adjustment	S_{FC}	S_{FE}	S_{GS}	bb
+10%	0.892	0.889	1.27	15.2
−10%	0.912	0.756	1.43	16.8

We use the maximum difference from the nominal value, 0.9 events, as an estimate of this systematic error.

5.5 Unknown Background

There exists the possiblility of the presence of additional backgrounds in the $J/\psi+\mu^{\pm}$ data that we have not accounted for. To check for the effect that an additional background would have on our scale factors we run a total of 5 sets of 200 Monte Carlos where we add an additional background which we allow to be as large as the expected B_c signal (50 events). For each set we choose a background linear in shape, but vary the forward fraction with the following values: 1.0, 0.75, 0.5, 0.25, 0.0. Table 4 contains the average values for our scale factors and $b\bar{b}$ background prediction for each set of Monte Carlos. The maximum deviation from the orignal $b\bar{b}$ background prediction is 3.4 events, which we assign as a source of systematic error.

6 $b\bar{b}$ Background Summary

Table 5 gives a summary of our sources of systematic error and the total systematic error which is obtained by adding all sources in quadrature. With the updated

Forward Fraction	S_{FC}	S_{FE}	S_{GS}	$b\bar{b}$
1.0	0.896	0.627	1.62	18.8
0.75	0.785	0.741	1.58	18.4
0.50	0.791	0.836	1.45	17.0
0.25	0.789	0.960	1.29	15.4
0.0	0.931	1.05	0.997	12.7

Table 4: Scale factors and $b\bar{b}$ predictions from the Monte Carlos with additional unknown backgrounds.

error the $b\bar{b}$ background is: 16.1 ± 2.1(stat.)± 5.7(syst.). Table 6 summarizes the $b\bar{b}$ predictions for the B_c signal region as well as the sideband regions.

Source	Value
Fit and Scaling Errors	4.3
Fitting Program Bias	0.6
J/Ψ Pseudo-Lifetime Cut	1.2
$J/\Psi+\mu$ Rate	0.5
B_c $\Delta\phi$ Shape	0.9
Unknown Background	3.4
Total Systematic	5.7

Table 5: Summary of contributions to systematic errors in $b\bar{b}$ background calculation.

7 Conclusion

We have performed a calculation of the $b\bar{b}$ background in the $B_c^\pm \rightarrow J/\psi + \mu^\pm + X$ decay channel. The calculation required two major corrections. First, calculation of a correction factor C_{Norm} to account for differences in $B^\pm$ production and $B^\pm \rightarrow J/\psi + K^\pm$ decay fraction between data and Pythia, allowing for normalization of the $b\bar{b}$ background using the $B^\pm \rightarrow J/\psi + K^\pm$ mass peak. Second, calculation of scale factors for the three Pythia production mechanisms so as to produce a Pythia sample with a $J/\psi+\mu^\pm$ $\Delta\phi$ distribution matching data, and therefore giving more accurate results in the forward direction, to which the B_c analysis is sensitive. The results of the two corrections are checked by looking at the $J/\psi+\mu^\pm$ mass distribution above $6.0 \mathrm{GeV/c^2}$ and with the requirement $\Delta\phi>\pi/2$. In these two regions there should be no B_c, and the prediction from $b\bar{b}$, DIF/PT and fake J/ψ events match both vertexed and unvertexed data well. With the corrections we calculate a $b\bar{b}$ background of 16.1 ± 2.1(stat.)± 5.7(syst.) events to be used in the B_c analysis.

Summary of Pythia $b\bar{b}$ background estimation for $p_t > 3.0$ GeV/c					
	$N_{Data}(B^{\pm})$		$N_{FC}(B^{\pm})$	$N_{FE}(B^{\pm})$	$N_{GS}(B^{\pm})$
B peak entries	755 ± 30		1293 ± 36	2688 ± 52	962 ± 31
			S_{FC}	S_{FE}	S_{GS}
Process dependent scale factors			0.90 ± 0.21	0.81 ± 0.37	1.36 ± 0.39
Mass window			A	B	C
Pythia $b\bar{b}$ background		N_{FC}	0	1	0
		N_{FE}	2	17	13
		N_{GS}	1	41	15
Predicted $b\bar{b}$ background			$0.7 \pm 0.4 \pm 0.1$	$16.1 \pm 2.1 \pm 5.7$	$7.1 \pm 1.3 \pm 1.8$

Table 6: Summary of $b\bar{b}$ background calculation. The mass windows are: A) $3.0 - 4.0$ GeV/c^2, B) $4.0 - 6.0$ GeV/c^2 (signal region), and C) $6.0 - 10.0$ GeV/c^2.

Appendix

A Study of Kinematic Variables for Seperation of QCD Processes

To fix the relative amounts of the QCD processes (FC, FE and GS) in Pythia, we fit Pythia to data (allowing the normalization of the QCD processes to float) using the distributions of one or more kinematic variables from the $b\bar{b}$ pair. To decide which variable(s) give the best seperation between QCD processes, we study the distributions for five different variables, broken up by QCD process. The variables are:

- $\Delta\phi$ - The azimuthal angle between the J/ψ and the third μ.
- $\Delta\eta$ - The difference between the pseudo-rapidity of J/ψ and the third μ.
- Δp_T - The difference between the maginitudes of the J/ψ p_T and the third μ p_T.
- $(p_T)_{J/\psi}$ - The J/ψ p_T.
- $(p_T)_{\mu}$ - The third μ p_T.

Once we have determined the best variable(s) for the tuning of the QCD processes, we will verify that those variables not used in the tuning procedure show reasonable agreement with data after the tuning procedure. Finally we will study the correlations of our variables in the hopes that we may see additional seperation for QCD processes when looking at two dimensional distributions.

A.1 Kinematic Varibles vs. QCD Processes

We study how well our variables seperate the QCD processes by taking the Pythia $b\bar{b}$ sample to be used in the tuning procedure, and plotting histograms for each of the five kinematic varibles broken up by QCD process. The results can be seen in Figure 19. We estimate the ability of these variables to seperate the QCD processes, by comparing the the mean and RMS values for each varible distribution, broken up by QCD process. For this comparison we estimate statistical errors based on the expected size of each QCD process in our data sample (about 200 events each) and apply the following formula, where N_i is the approximate number of each QCD process in data and RMS_i is the predicted RMS value for each process:

$$E_{mean}, E_{RMS} = \frac{1}{\sqrt{N_i}} \times RMS_i$$

The results can be seen in Figure 20 and Figure 21. $\Delta\phi$ is the only variable that shows statistically significant seperation between all three QCD processes, and we choose it to tune the Pythia to data.

A.2 Validation of Non-tuned Kinematic Variables

Having tuned the the Pythia sample by fitting the $\Delta\phi$ to data by adjusting the relative amounts of FC, FE and GS in Pythia, we now study the variables that were not used in the tuning procedure, and make sure they agree well with data. Figure 22 contains histograms comparing the predicted $\Delta\eta$, Δp_T, $(p_T)_{J/\psi}$ and $(p_T)_\mu$ distributions to data. The predicted distributions consists primarily of our tuned $b\bar{b}$ events from Pythia (with smaller contributions from fake muon, fake J/ψ and B_c events). We see good agreement for $\Delta\eta$ and $(p_T)_\mu$. For $(p_T)_{J/\psi}$ and Δp_T it appears that the predicted distributions are shifted towards lower p_T. We hypothesize that this is due to trigger turn on effects that are not modeled in Pythia, but exist in data. To check this hypothesis we increase the p_T requirement on our J/ψ legs from 1.5 GeV/c (the trigger requirement) to 1.8 GeV/c to cut out the turn on. The distributions, shown in Figure 23, show better agreement with data. In the future, we hope to fix this problem by modeling trigger efficiencies in Pythia.

A.3 Variable Correlations with $\Delta\phi$

While $\Delta\eta$, Δp_T, $(p_T)_{J/\psi}$ and $(p_T)_\mu$ distributions for the QCD processes do not show seperation significant enough for tuning the Pythia sample, it may be true that two dimensional distribution of the previously mentioned variables with $\Delta\phi$ could be used to improve our one dimensional $\Delta\phi$ fit. Figure 24, Figure 25, Figure 26 and Figure 27 show the distributions for the different QCD processes broken up into $\Delta\phi$ slices. For some of the $\Delta\phi$ bins any conclusion is limited by the statistics of the Pythia sample, but it appears that none of the $\Delta\phi$ correlations would significantly improve our fitting procedure.

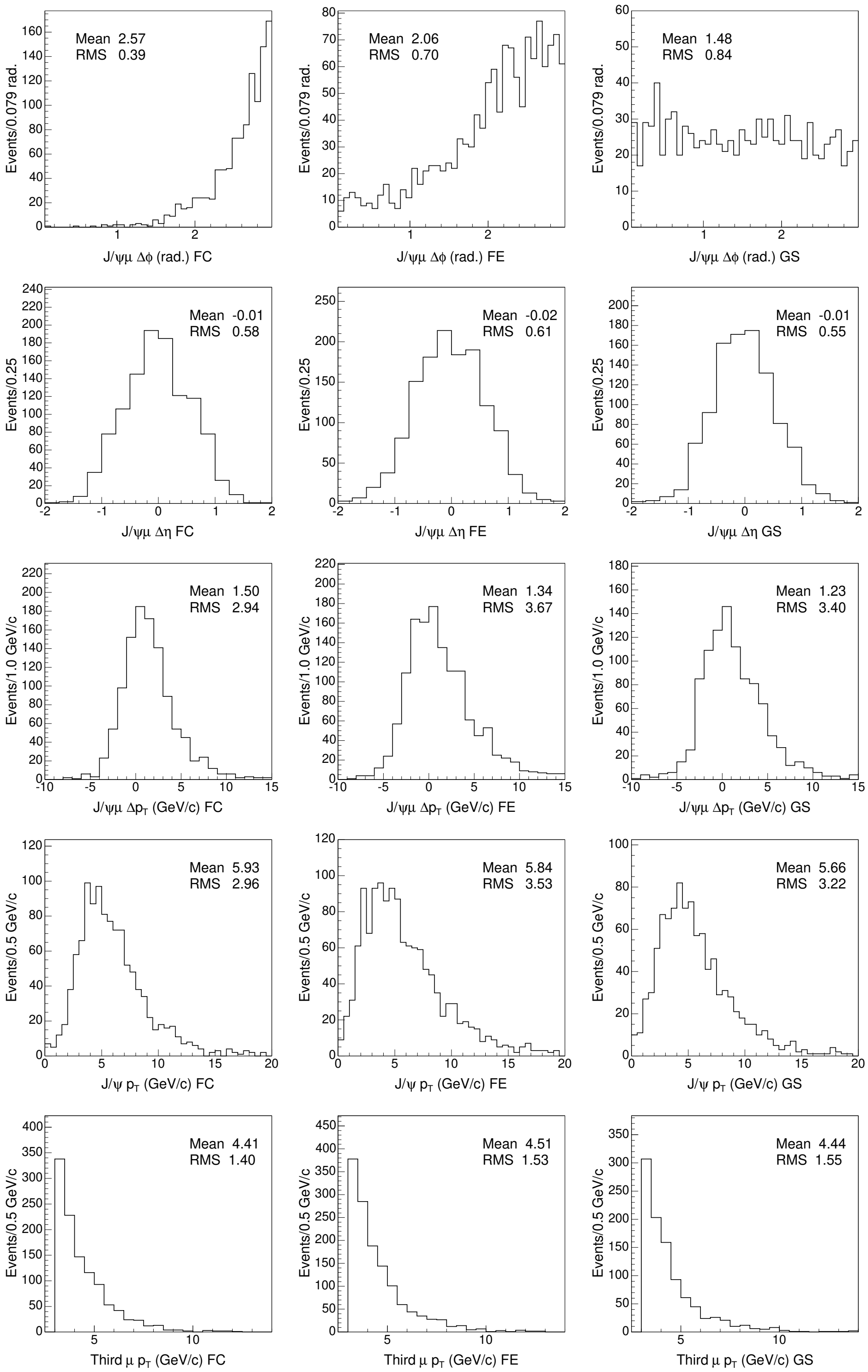

Figure 19: Columns contain the three QCD processes in Pythia, from left to right: FC, FE, GS. Rows contain the distributions for the variables we are studying, from top to bottom: $\Delta\phi$, $\Delta\eta$, Δp_T, $(p_T)_{J/\psi}$, $(p_T)_\mu$.

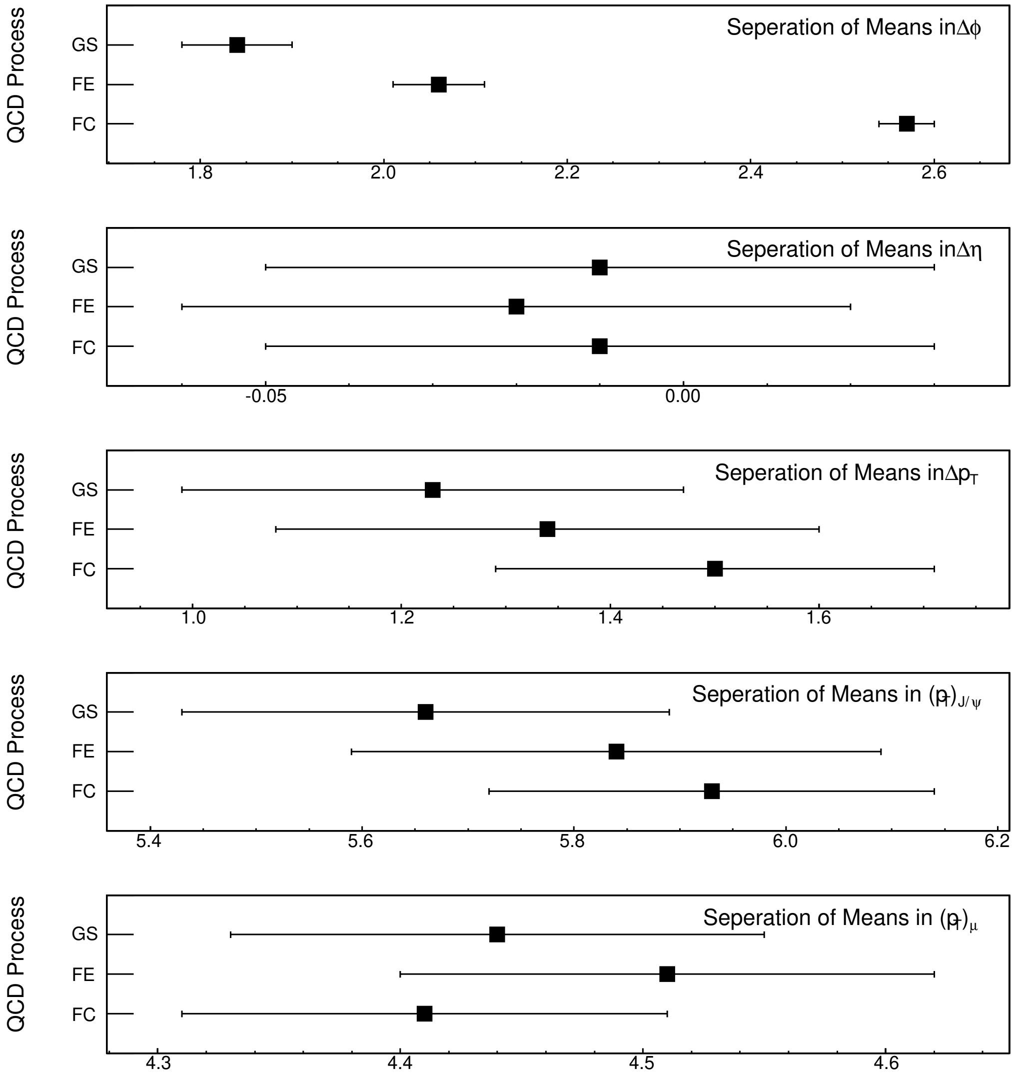

Figure 20: Comparison of the expected seperation in data of the mean values of variables of interest for different QCD processes. From top to bottom: $\Delta\phi$, $\Delta\eta$, Δp_T, $(\mathrm{p}_T)_{J/\psi}$, $(\mathrm{p}_T)_{\mu}$.

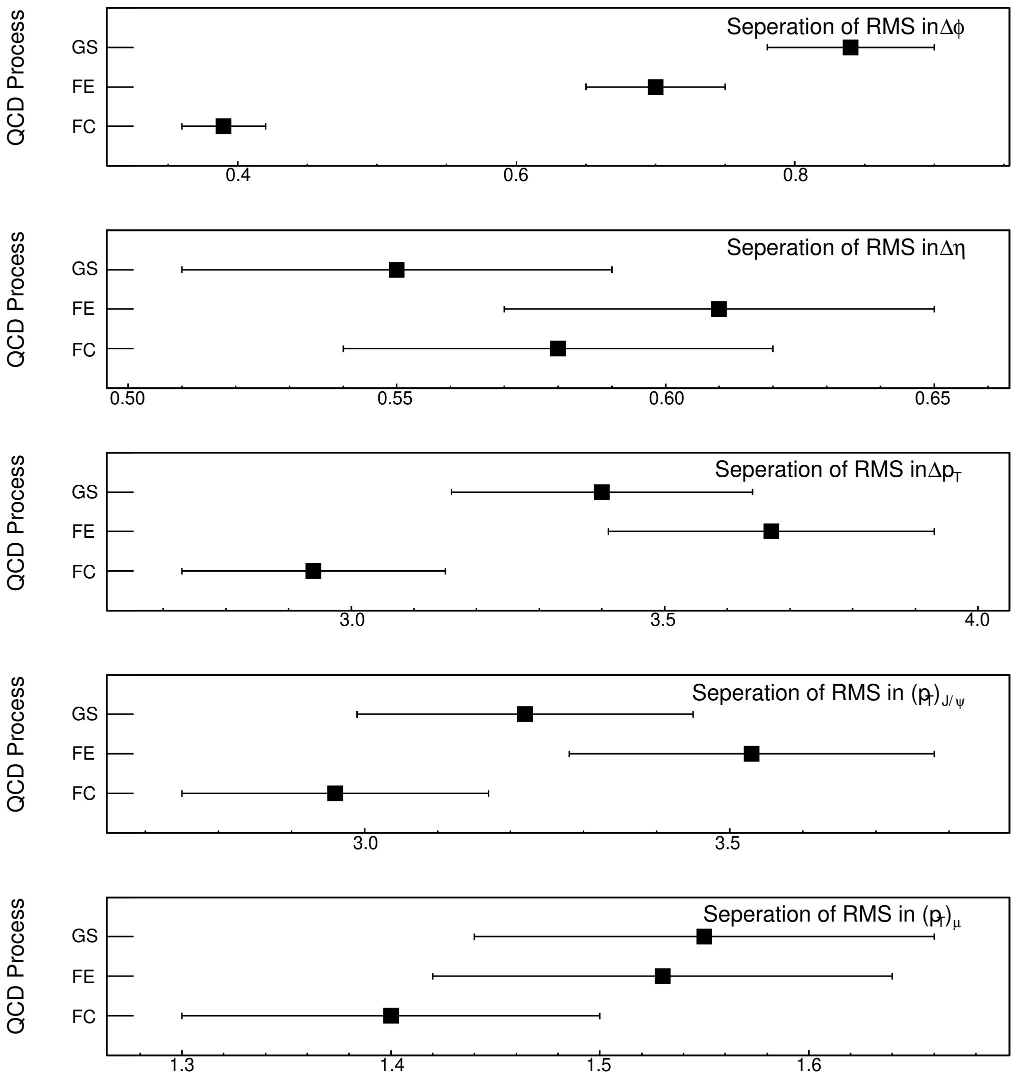

Figure 21: Comparison of the expected seperation in data of the RMS values of variables of interest for different QCD processes. From top to bottom: $\Delta\phi$, $\Delta\eta$, Δp_T, $(\mathrm{p}_T)_{J/\psi}$, $(\mathrm{p}_T)_{\mu}$.

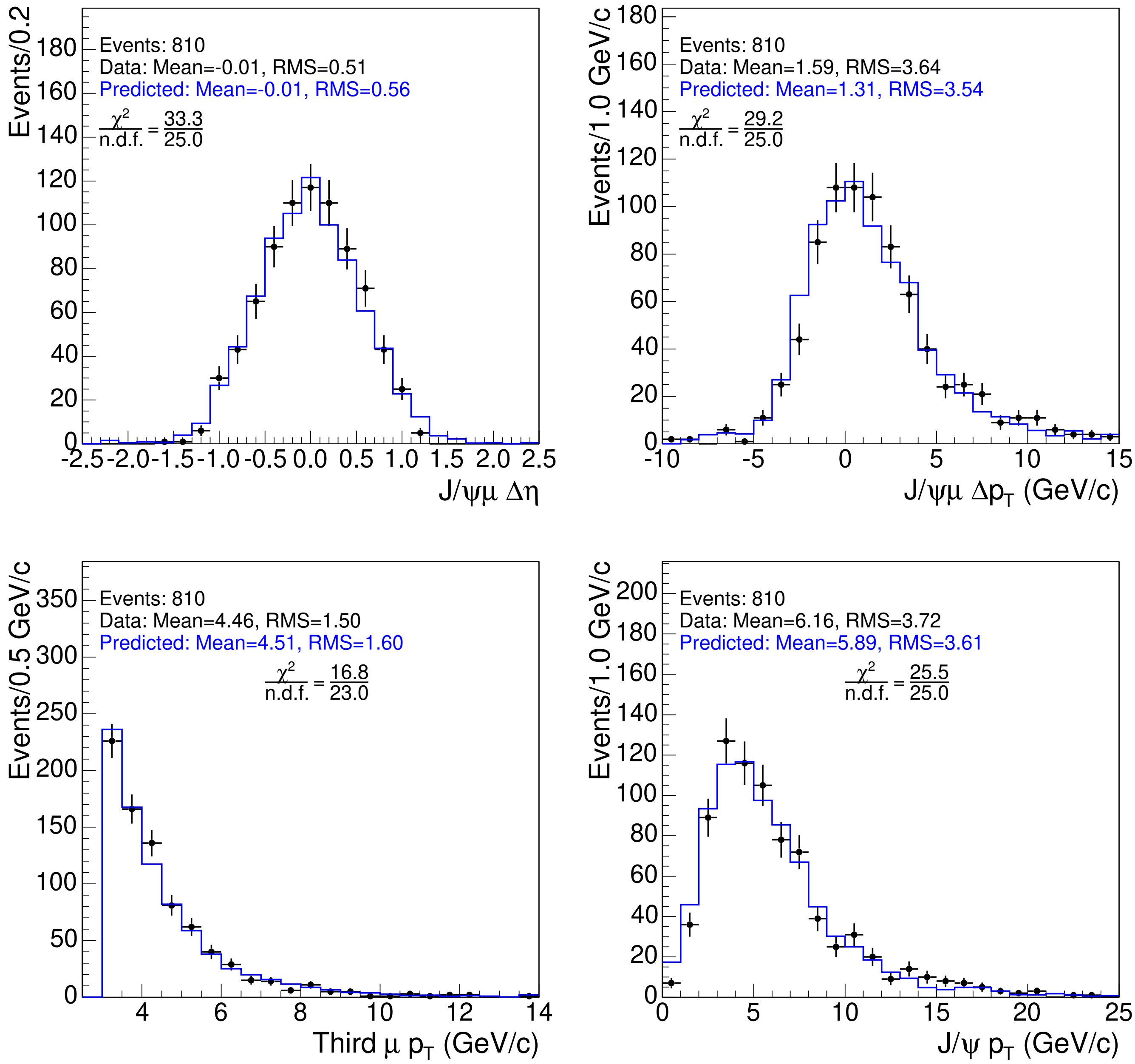

Figure 22: Predicted distributions (blue) compared to data (black) for: $\Delta\eta$ (top left), Δp_T (top right), $(\mathrm{p}_T)_\mu$ (bottom left) and $(\mathrm{p}_T)_{J/\psi}$ (bottom right).

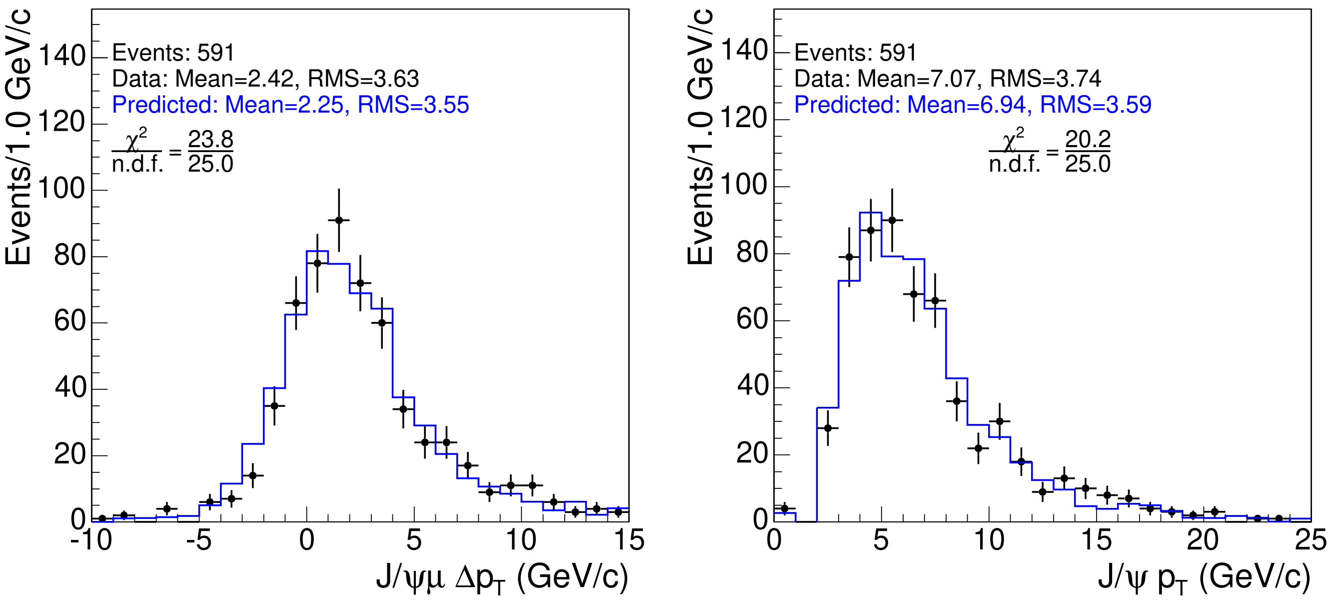

Figure 23: Predicted distributions (blue) compared to data (black) with $p_T > 1.8$ GeV reqirement for J/ψ legs to remove trigger turn on from data. Left: Δp_T. Right: $(\mathrm{p}_T)_{J/\psi}$.

To verify that our one dimensional tuning using $\Delta\phi$ gives reasonable results for correlations vs. $\Delta\phi$ we plot the predicted and data distributions for $\Delta\eta$, Δp_T, $(\mathrm{p}_T)_{J/\psi}$ and $(\mathrm{p}_T)_\mu$ broken up into $\Delta\phi$ slices. These histograms can be seen in Figure 28, Figure 29, Figure 30 and Figure 31. The agreement is acceptable within statistics.

A.4 Summary

We have studied the variables: $\Delta\phi$, $\Delta\eta$, Δp_T, $(\mathrm{p}_T)_{J/\psi}$ and $(\mathrm{p}_T)_\mu$, and determined that only $\Delta\phi$ shows enough seperation between the QCD processes to be used to tune our Pythia sample. Having tuned the Pythia sample by fitting the $\Delta\phi$ distribution to data, we verified that the predicted distributions for those variables not used in the tuning agree with data. We saw some disagreement in the $(\mathrm{p}_T)_{J/\psi}$ distribution but we believe this to be a trigger effect and hope to model it in the future. Finally we looked at two dimensional distributions of our variables with $\Delta\phi$ and saw no additional power to seperate the QCD processes and good agreement between predicted and data distributions, confirming our choice of $\Delta\phi$ for the tuning of Pythia.

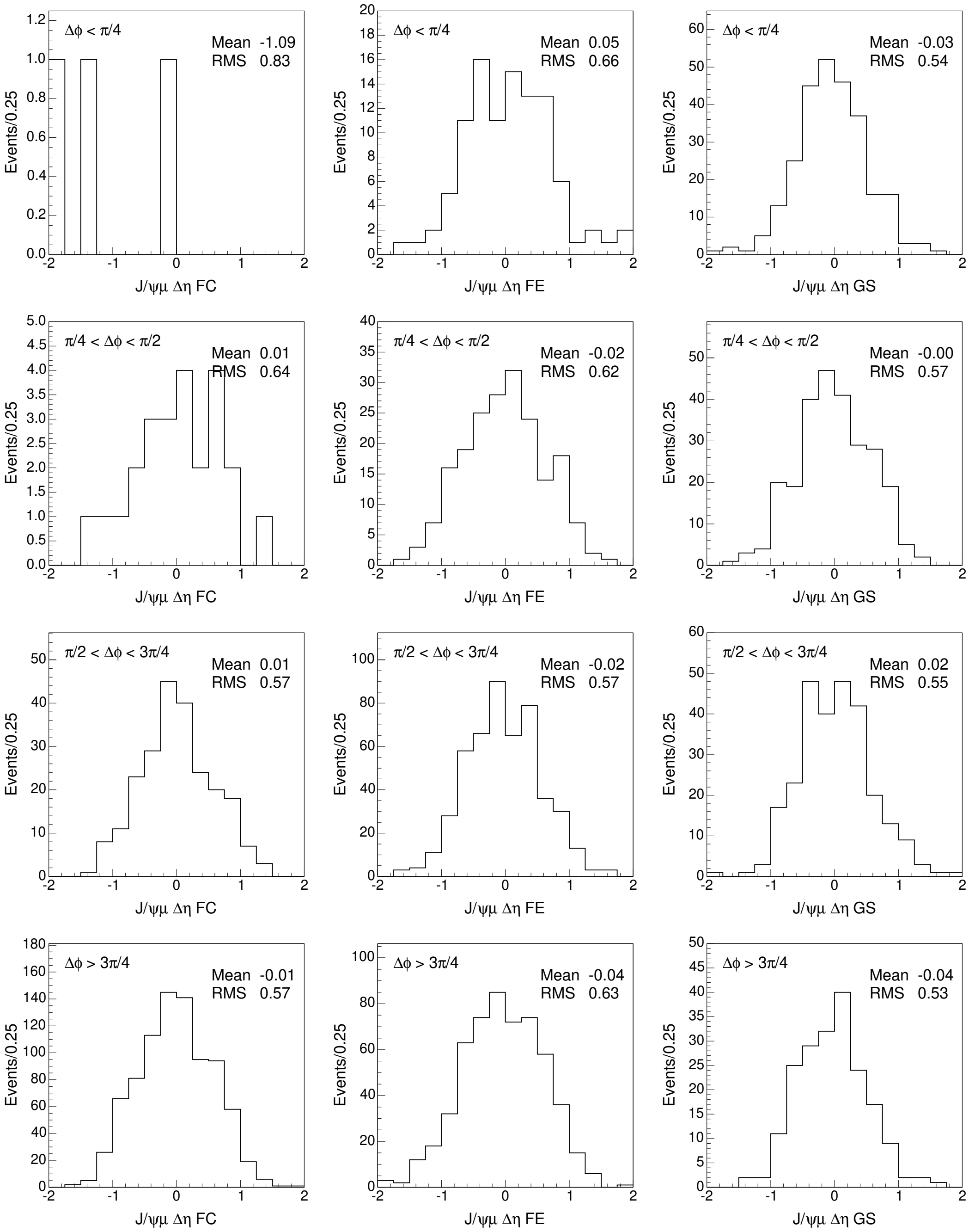

Figure 24: Columns contain the three QCD processes in Pythia, from left to right: FE, FC, GS. Rows contain the distributions for $\Delta\eta$ broken into $\Delta\phi$ slices, from top to bottom: $\Delta\phi < \pi/4$, $\pi/4 < \Delta\phi < \pi/2$, $\pi/2 < \Delta\phi < 3\pi/4$ and $\Delta\phi > 3\pi/4$

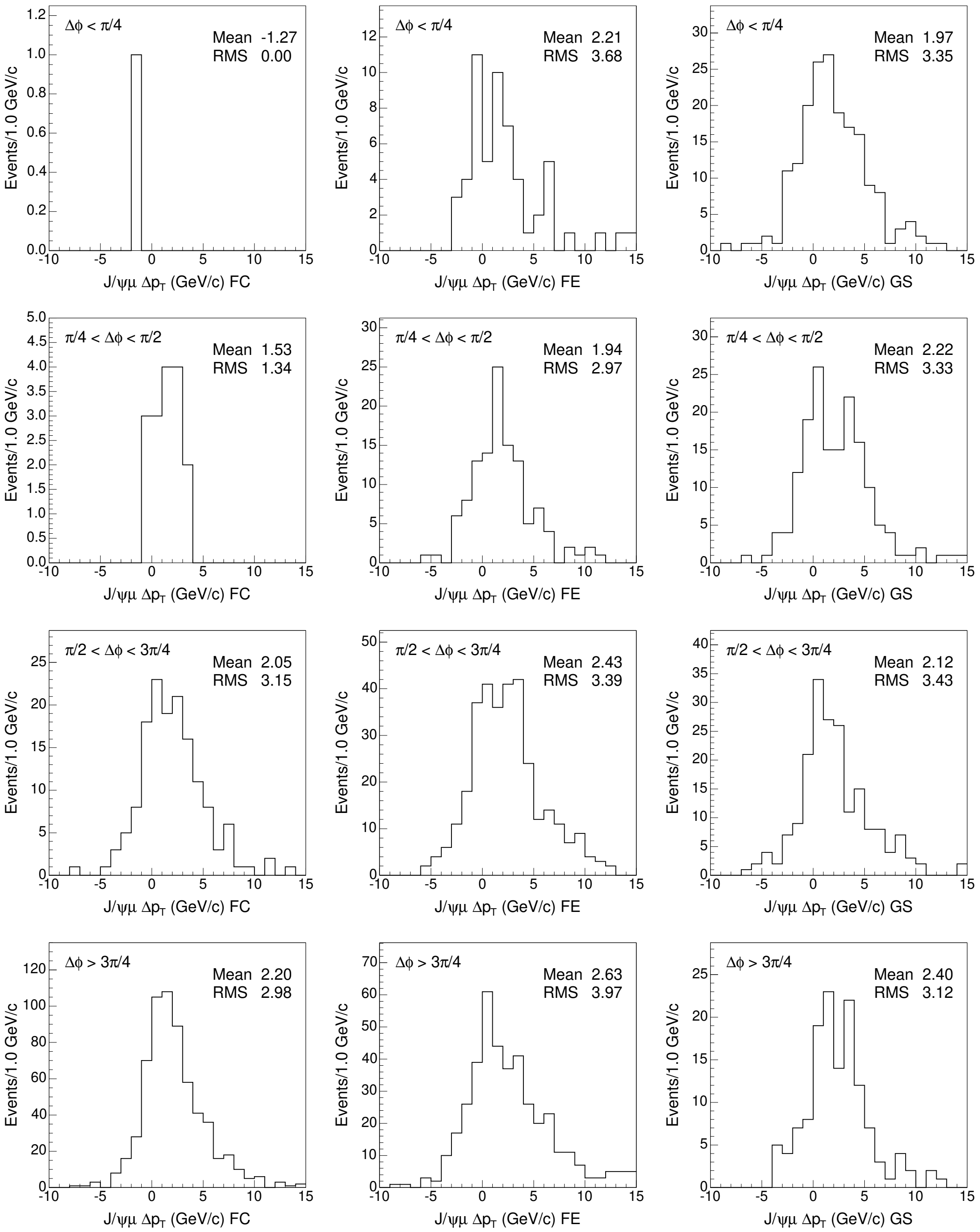

Figure 25: Columns contain the three QCD processes in Pythia, from left to right: FE, FC, GS. Rows contain the distributions for Δp_T broken into $\Delta\phi$ slices, from top to bottom: $\Delta\phi < \pi/4$, $\pi/4 < \Delta\phi < \pi/2$, $\pi/2 < \Delta\phi < 3\pi/4$ and $\Delta\phi > 3\pi/4$

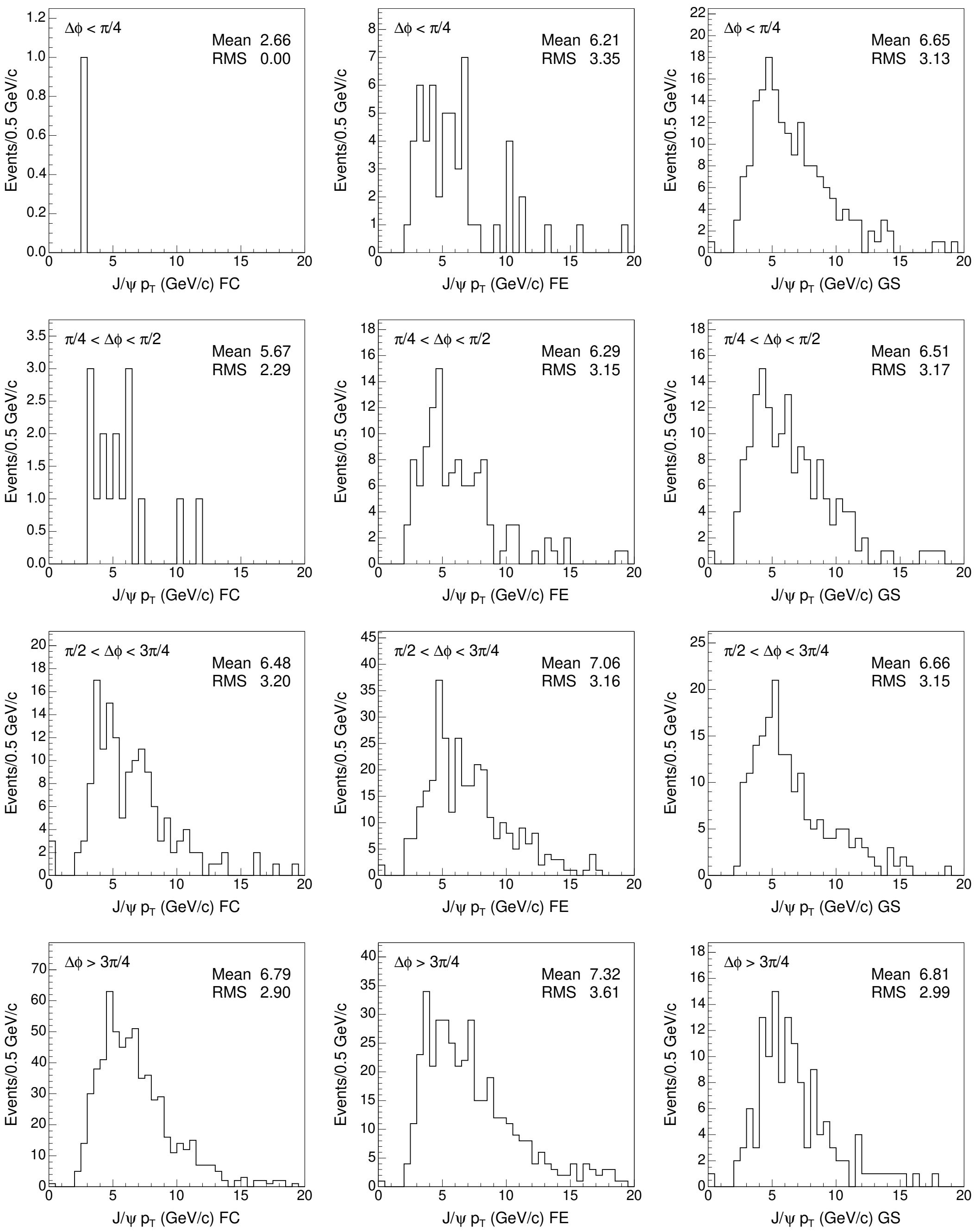

Figure 26: Columns contain the three QCD processes in Pythia, from left to right: FE, FC, GS. Rows contain the distributions for $(\mathrm{p}_T)_{J/\psi}$ broken into $\Delta\phi$ slices, from top to bottom: $\Delta\phi < \pi/4$, $\pi/4 < \Delta\phi < \pi/2$, $\pi/2 < \Delta\phi < 3\pi/4$ and $\Delta\phi > 3\pi/4$

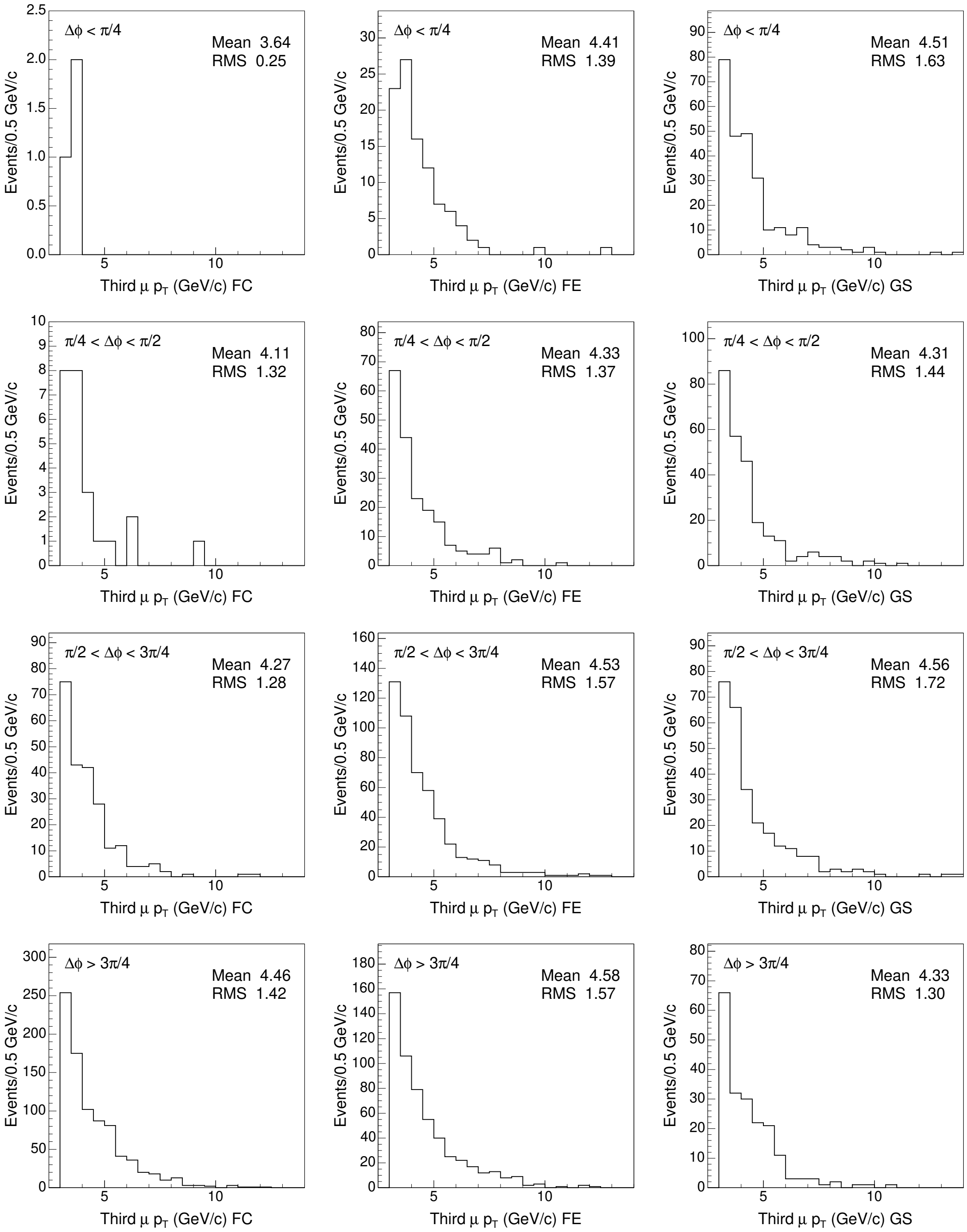

Figure 27: Columns contain the three QCD processes in Pythia, from left to right: FE, FC, GS. Rows contain the distributions for $(p_T)_\mu$ broken into $\Delta\phi$ slices, from top to bottom: $\Delta\phi < \pi/4$, $\pi/4 < \Delta\phi < \pi/2$, $\pi/2 < \Delta\phi < 3\pi/4$ and $\Delta\phi > 3\pi/4$

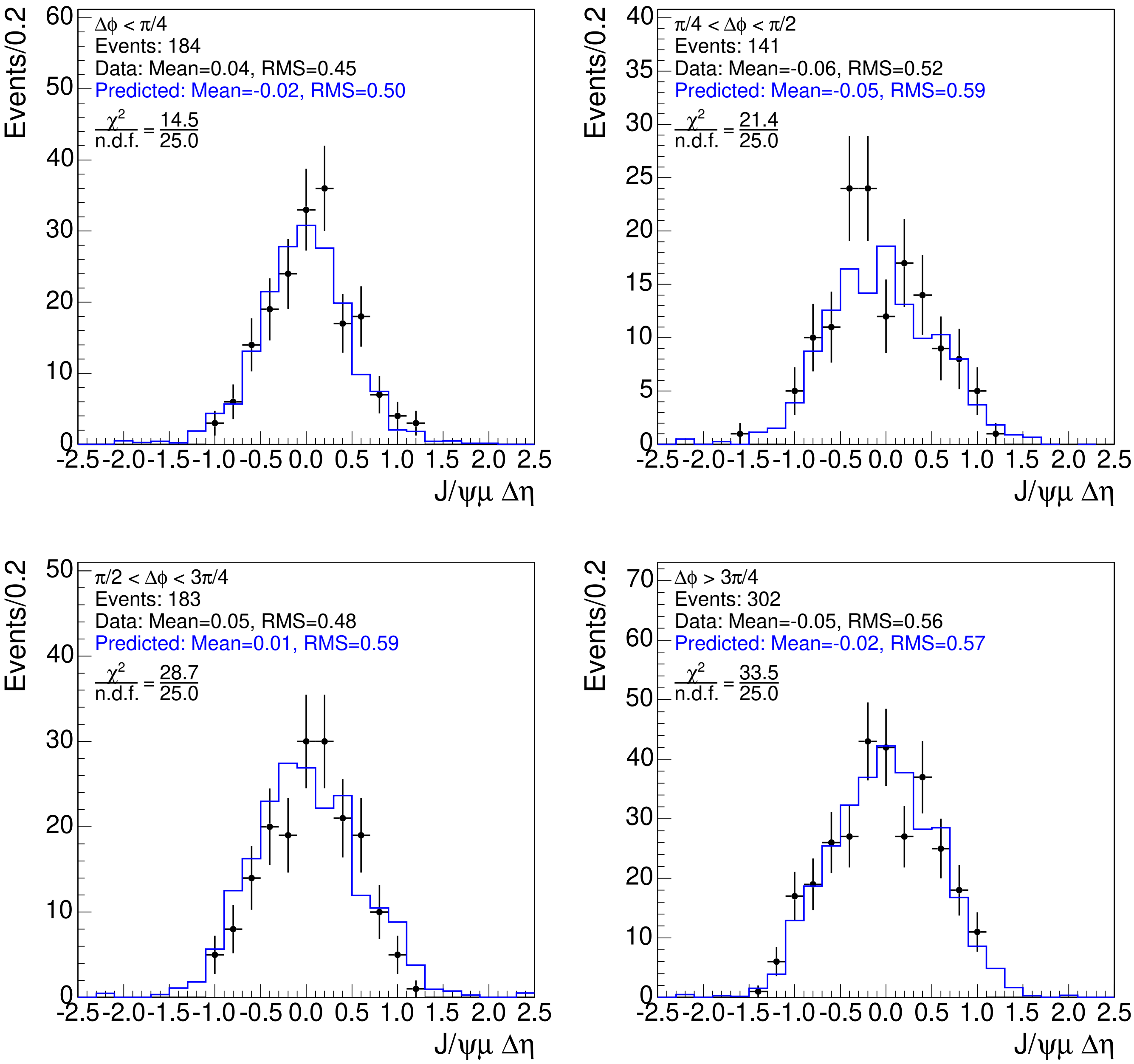

Figure 28: $\Delta\eta$ for predicted (blue) and data (black) broken into $\Delta\phi$ slices. Top Left: $\Delta\phi < \pi/4$. Top Right: $\pi/4 < \Delta\phi < \pi/2$. Bottom Left: $\pi/2 < \Delta\phi < 3\pi/4$. Bottom Right: $\Delta\phi > 3\pi/4$.

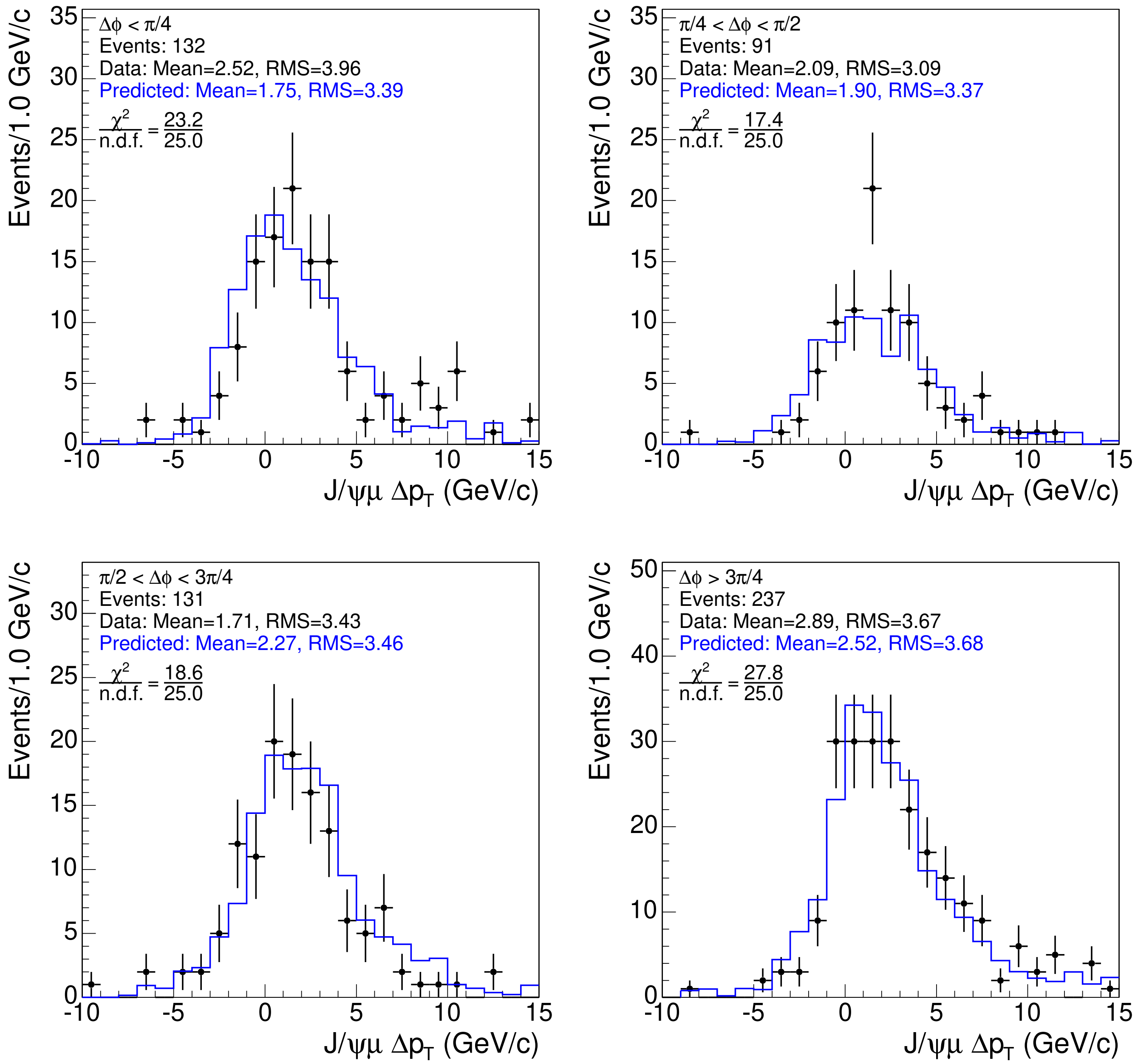

Figure 29: Δp_T for predicted (blue) and data (black) broken into $\Delta\phi$ slices. Top Left: $\Delta\phi < \pi/4$. Top Right: $\pi/4 < \Delta\phi < \pi/2$. Bottom Left: $\pi/2 < \Delta\phi < 3\pi/4$. Bottom Right: $\Delta\phi > 3\pi/4$.

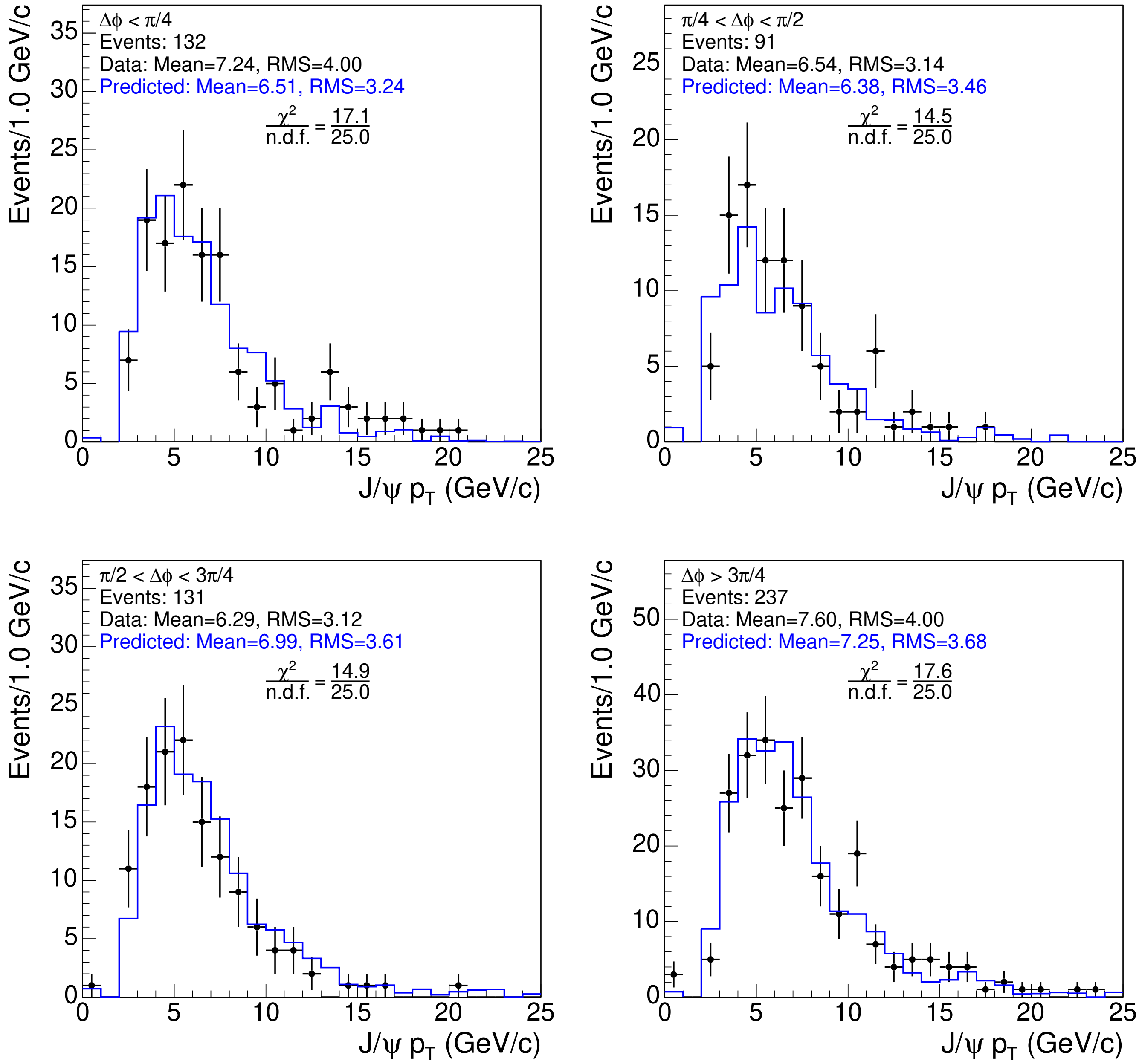

Figure 30: J/ψ p_T for predicted (blue) and data (black) broken into $\Delta\phi$ slices. Top Left: $\Delta\phi < \pi/4$. Top Right: $\pi/4 < \Delta\phi < \pi/2$. Bottom Left: $\pi/2 < \Delta\phi < 3\pi/4$. Bottom Right: $\Delta\phi > 3\pi/4$.

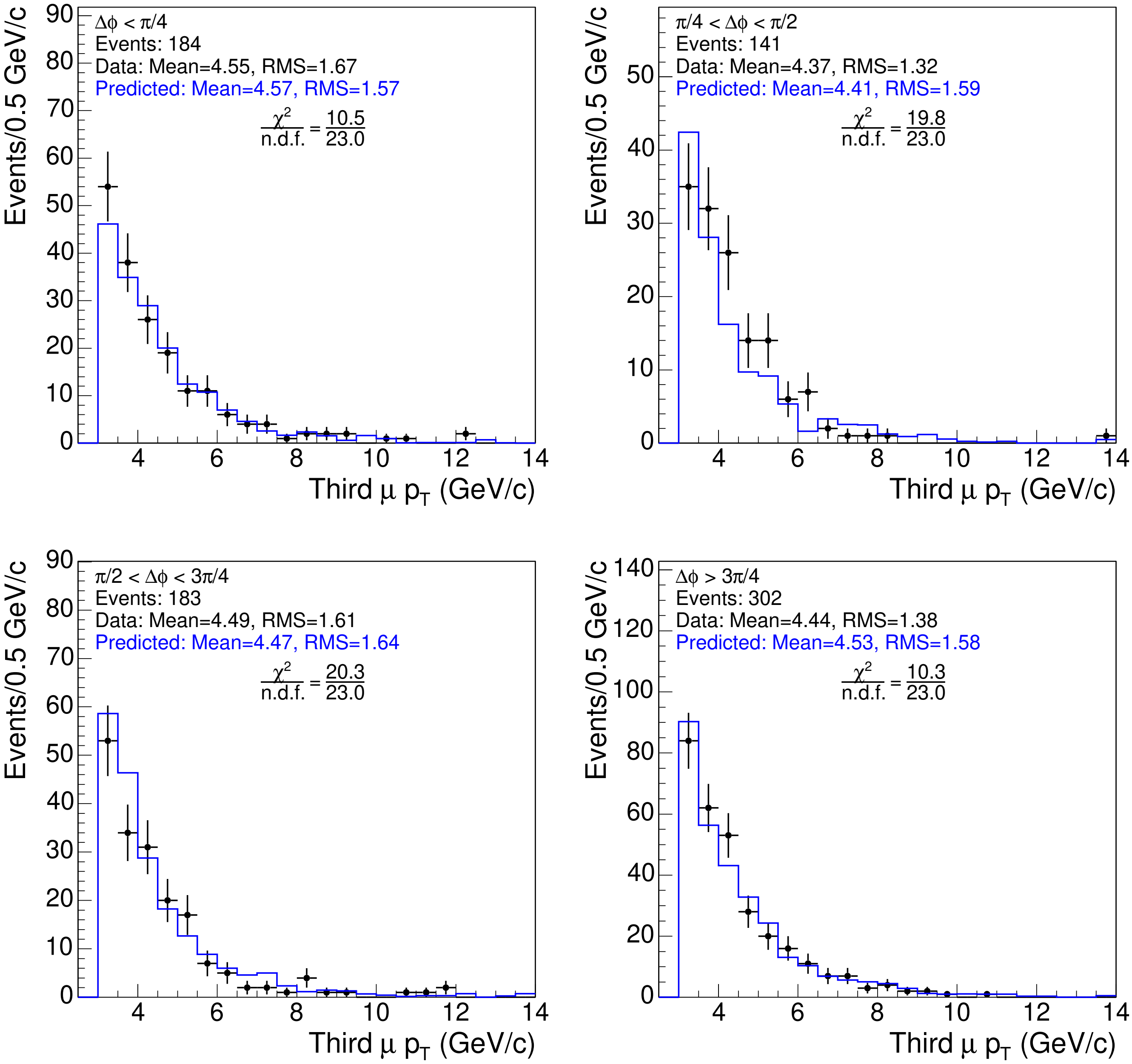

Figure 31: Third μ p$_T$ for predicted (blue) and data (black) broken into $\Delta\phi$ slices. Top Left: $\Delta\phi < \pi/4$. Top Right: $\pi/4 < \Delta\phi < \pi/2$. Bottom Left: $\pi/2 < \Delta\phi < 3\pi/4$. Bottom Right: $\Delta\phi > 3\pi/4$.

References

[1] S. Eidelman et al. (Particle Data Group), Physics Letters B592, 1 2004.

[2] K. Lannon, "A Measurement of B Hadron Correlations In $p\bar{p}$ Collisions at $\sqrt{s} =$ 1.8 TeV" CDF Thesis (2003).

[3] George Pope, Turgun Nigmanov and Paul Shepard, "Study of $B_c^{\pm} \rightarrow \mathrm{J}/\psi + \mu^{\pm}$ in Run II data" CDF Note 6956 (2004).

[4] W. Kwong and J. Rosner, Phys. Rev. D44, p212, 1991.

[5] Kevin Lannon and Tony Affolder, "Measurement of Bottom Quark-Antiquark Azimuthal Production Correlations in Proton-Antiproton Collisions at $\sqrt{s} = 1.8$ TeV" CDF Note 7253 (2004).